

# Physics-Compliant Modeling and Optimization of MIMO Systems Aided by Microwave Linear Analog Computers

Matteo Nerini, *Member, IEEE*, Bruno Clerckx, *Fellow, IEEE*

**Abstract**—Microwave linear analog computer (MiLAC) has emerged as a promising architecture for implementing linear multiple-input multiple-output (MIMO) processing in the analog domain, with radio frequency (RF) signals. Existing studies on MiLAC-aided communications rely on idealized channel models and neglect antenna mutual coupling. However, since MiLAC performs processing at RF, mutual coupling becomes critical and alters the implemented operation, not only the channel characteristics. In this paper, we develop a physics-compliant model for MiLAC-aided MIMO systems accounting for mutual coupling with multiport network theory. We derive end-to-end system models for scenarios with MiLACs at the transmitter, the receiver, or both, showing how mutual coupling impacts the linear transformation implemented by the MiLACs. Furthermore, we formulate and solve a mutual coupling aware MiLAC optimization problem, deriving a closed-form globally optimal solution that maximizes the received signal power. We establish the fundamental performance limits of MiLAC with mutual coupling, and derive three analytical results. First, mutual coupling is beneficial in MiLAC-aided systems, on average. Second, with mutual coupling, MiLAC performs as digital architectures equipped with a matching network, while having fewer RF chains. Third, with mutual coupling, MiLAC always outperforms digital architectures with no matching network. Numerical simulations confirm our theoretical findings.

**Index Terms**—Beamforming, gigantic multiple-input multiple-output (MIMO), microwave linear analog computer (MiLAC), mutual coupling

## I. INTRODUCTION

The unprecedented growth of mobile data traffic and the requirements anticipated for sixth-generation (6G) wireless networks demand transformative shifts in wireless system design [1]. Among the key technologies enabling these capabilities, gigantic MIMO has emerged, exploiting large antenna arrays to increase spectral efficiency and spatial multiplexing gains [2]. Whereas fifth-generation (5G) systems employ massive MIMO arrays with tens of antennas, 6G visions push toward gigantic MIMO, involving hundreds or even thousands of antennas [3]. However, scaling conventional digital MIMO architectures to such dimensions introduces prohibitive hardware costs and computational burdens. Each antenna typically requires a dedicated RF chain with high-resolution analog-to-digital converters (ADCs) and digital-to-analog converters

(DACs), and real-time digital signal processing whose complexity scales rapidly with array size.

To address these challenges, researchers have explored a range of alternative architectures that reduce reliance on digital processing. Hybrid analog-digital beamforming distributes signal processing between baseband digital and RF analog domains, lowering the number of RF chains while retaining performance [4], [5]. Similarly, technologies such as reconfigurable intelligent surfaces (RISs) and dynamic metasurface antennas (DMAs) steer or shape electromagnetic (EM) waves in the analog domain [6], [7]. Parallel to these developments, there has been a revival of analog computing paradigms for communications, motivated by their potential for ultra-fast and highly parallel computation. The resurgence is driven by advances in analog hardware, including metasurfaces and resistive memory arrays that allow certain operations to be mapped directly onto physical analog structures [8], [9].

In this context, MiLAC has recently been proposed as a class of analog computers capable of processing microwave signals directly in the analog domain [10]. A MiLAC is a multiport microwave network made of (possibly tunable) impedance elements that linearly map input signals to outputs, effectively implementing linear transformations and beamforming tasks without extensive digital processing. Early studies showed that a MiLAC can compute linear minimum mean square error (LMMSE) estimators and matrix inversions with computational complexity scaling quadratically rather than cubically, enabling orders-of-magnitude reductions compared to digital computing [10]. Building on this foundation, MiLAC-aided beamforming has been introduced as a way of performing precoding and combining entirely at RF, in the analog domain [11]. MiLAC-aided beamforming can achieve flexibility and performance comparable to digital beamforming while requiring significantly fewer RF chains, lower ADCs/DACs resolution, and reduced digital processing.

Subsequent work has further studied MiLAC-aided communications. The capacity of MiLAC-aided MIMO systems has been characterized under the constraints of lossless and reciprocal RF components, and analytically shown to match that of digital beamforming systems [12]. Efficient MiLAC architectures with reduced circuit complexity have been developed by using graph theory, addressing practical implementation challenges associated with fully-connected microwave networks [13]. The performance limits of MiLAC in multi-user systems have been investigated [14], [15]. While a lossless and reciprocal MiLAC cannot exactly match the performance of

This work has been supported in part by UKRI under Grant EP/Y004086/1, EP/X040569/1, EP/Y037197/1, EP/X04047X/1, EP/Y037243/1.

Matteo Nerini and Bruno Clerckx are with the Department of Electrical and Electronic Engineering, Imperial College London, SW7 2AZ London, U.K. (e-mail: m.nerini20@imperial.ac.uk; b.clerckx@imperial.ac.uk).

digital beamforming [14], hybrid MiLAC-digital beamforming can achieve maximum performance with only  $K$  RF chains, with  $K$  being the number of users [15], in contrast to hybrid analog-digital beamforming requiring  $2K$  RF chains [4]. Moreover, the problem of low-complexity channel estimation in MiLAC-aided systems has been addressed in [16].

Existing work on MiLAC-aided communications has largely relied on idealized channel models [10]-[16]. In particular, prior studies assume perfectly matched antennas and neglect antenna mutual coupling, which is particularly strong in tightly packed antenna arrays. While these assumptions enable analytical tractability and provide valuable insights into the fundamental potential of MiLAC, they neglect EM non-idealities, such as mutual coupling, that inevitably arise in practical implementations of multi-antenna devices.

Mutual coupling between antenna elements arises when the EM signal radiated by an antenna induces currents on neighboring antennas, thereby changing the EM signals they radiate. These effects are known from classical MIMO theory to influence the channel characteristics, introducing correlation between antenna ports and affecting the achievable performance. Mutual coupling has been extensively studied and modeled in conventional digital MIMO systems using multiport network theory, either through impedance parameters [17], [18], [19], or scattering parameters [20], [21]. Recent works also explored the role of mutual coupling in RIS [22], [23], [24], [25] and DMA [26]. However, the role of mutual coupling in MiLAC-aided systems is fundamentally different and potentially more critical. In MiLAC-aided systems, beamforming is performed directly in the EM domain through a reconfigurable microwave network, rather than being carried out in baseband. Consequently, mutual coupling does not merely perturb the channel, but directly interacts with the analog processing of the MiLAC, influencing the implemented linear operator and the resulting end-to-end system behavior.

This observation motivates the need for a rigorous and physically grounded modeling for MiLAC-aided systems that explicitly accounts for mutual coupling effects. Understanding how coupling modifies the effective MiLAC operation and impacts beamforming is essential for assessing performance limits and guiding practical design. In this paper, we fill this gap by developing a comprehensive model of MiLAC-aided MIMO systems in the presence of antenna mutual coupling, and proposing a mutual coupling aware optimization algorithm for MiLAC. Specifically, the contributions of this paper are as follows.

*First*, we develop a rigorous physics-compliant model for MIMO systems aided by MiLAC through multiport network theory, explicitly accounting for antenna mutual coupling. We derive end-to-end system models for three cases where: *i*) only the transmitter is equipped with a MiLAC (Section III), *ii*) only the receiver is equipped with a MiLAC (Section IV), and *iii*) both the transmitter and the receiver are equipped with a MiLAC (Section V). For each of these cases, we show how mutual coupling alters the impact of MiLAC on the wireless channel.

*Second*, we formulate and solve an optimization problem for MiLAC in the presence of antenna mutual coupling (Sec-

tion VI). Considering a multiple-input single-output (MISO) system with MiLAC at the transmitter, we derive a global optimal solution that maximizes the received signal power. Furthermore, we obtain closed-form expressions for the maximum achievable performance and for its average in the presence of uncorrelated fading channels. Analytical results show that MiLAC with mutual coupling achieves better average performance than with no mutual coupling.

*Third*, we compare MiLAC-aided beamforming with digital beamforming by examining two possible digital architectures: one equipped with a matching network (or decoupling network) and one without it (Section VII). Comparing the optimal performance of MiLAC-aided beamforming and digital beamforming, we derive the following two analytical results: *i*) MiLAC achieves the same performance as digital beamforming with a matching network, for any channel realization. *ii*) in the presence of mutual coupling, MiLAC achieves better performance than digital beamforming without a matching network, for any channel realization.

*Fourth*, we validate the presented modeling and optimization algorithm through numerical simulations (Section VIII). Numerical results confirm that the proposed MiLAC optimization algorithm achieves the derived performance upper bounds, demonstrating its global optimality. We study the impact of mutual coupling on MiLAC-aided systems and conventional digital systems, numerically validating all our theoretical insights, namely that mutual coupling is beneficial in MiLAC-aided systems and that MiLAC outperforms digital beamforming with no matching network in the presence of mutual coupling.

*Notation*: Vectors and matrices are denoted with bold lower and bold upper letters, respectively. Scalars are represented with letters not in bold font.  $\Re\{a\}$ ,  $\Im\{a\}$ , and  $|a|$  refer to the real part, imaginary part, and absolute value of a complex scalar  $a$ , respectively.  $\mathbf{a}^T$ ,  $\mathbf{a}^H$ ,  $[\mathbf{a}]_i$ , and  $\|\mathbf{a}\|$  refer to the transpose, conjugate transpose,  $i$ th element, and  $l_2$ -norm of a vector  $\mathbf{a}$ , respectively.  $\mathbf{A}^T$ ,  $\mathbf{A}^H$ ,  $[\mathbf{A}]_{i,k}$ ,  $[\mathbf{A}]_{i,:}$ , and  $[\mathbf{A}]_{:,k}$  refer to the transpose, conjugate transpose,  $(i,k)$ th element,  $i$ th row, and  $k$ th column of a matrix  $\mathbf{A}$ , respectively.  $[\mathbf{A}]_{\mathcal{I},\mathcal{K}}$  refers to the submatrix of  $\mathbf{A}$  obtained by selecting the rows and columns indexed by the elements of the sets  $\mathcal{I}$  and  $\mathcal{K}$ , respectively.  $\mathbb{R}$  and  $\mathbb{C}$  denote the real and complex number sets, respectively.  $j = \sqrt{-1}$  denotes the imaginary unit.  $\mathbf{I}$  and  $\mathbf{0}$  denote the identity matrix and the all-zero matrix with appropriate dimensions.  $\mathbf{A} \succcurlyeq \mathbf{B}$  means that  $\mathbf{A} - \mathbf{B}$  is positive semi-definite.

## II. MODELING A MIMO SYSTEM

To introduce the necessary theoretical tools and the quantities in the considered wireless systems, we first model a conventional digital MIMO system, where each antenna is directly connected to an RF chain. The transmitting RF chains are modeled through voltage generators with their series impedance  $Z_0$ , e.g.,  $Z_0 = 50 \Omega$ , while the receiving RF chains are modeled as loads  $Z_0$ , assuming that their input impedances are perfectly matched. Such a MIMO system is represented in Fig. 1, where we have  $N_T$  transmitting antennas and  $N_R$  receiving antennas.

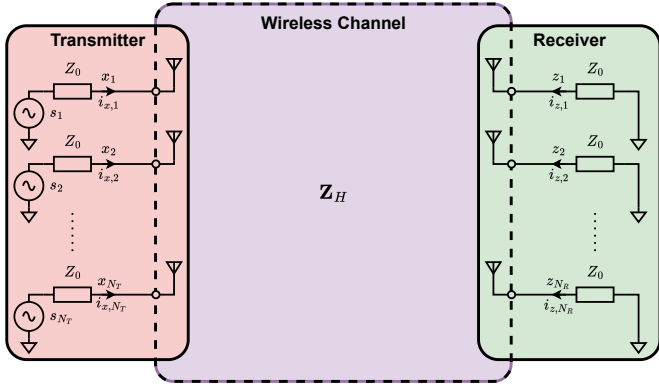


Fig. 1. Model of a MIMO system.

We denote the voltages at the voltage generators as  $\mathbf{s} \in \mathbb{C}^{N_T \times 1}$ , the voltages and currents at the transmitting antennas as  $\mathbf{x} \in \mathbb{C}^{N_T \times 1}$  and  $\mathbf{i}_x \in \mathbb{C}^{N_T \times 1}$ , and the voltages and currents at the receiver as  $\mathbf{z} \in \mathbb{C}^{N_R \times 1}$  and  $\mathbf{i}_z \in \mathbb{C}^{N_R \times 1}$ , as in Fig. 1. The received signal  $\mathbf{z}$  is related to the transmitted signal  $\mathbf{s}$  by

$$\mathbf{z} = \mathbf{H}\mathbf{s}, \quad (1)$$

where  $\mathbf{H} \in \mathbb{C}^{N_R \times N_T}$  is the wireless channel matrix between the transmitter and receiver. In the remainder of this section, our goal is to characterize  $\mathbf{H}$  through rigorous multiport network analysis, recalling what was done in classical MIMO literature [17], [18], [19], [20], [21].

#### A. Model With Mutual Coupling

To derive  $\mathbf{H}$ , we first study the relationships between the electrical quantities at the wireless channel, the transmitter, and the receiver, and then solve a system of linear equations involving these relationships. We model the wireless channel as a giant  $(N_T + N_R)$ -port network, which can be described by its impedance matrix  $\mathbf{Z}_H \in \mathbb{C}^{(N_T + N_R) \times (N_T + N_R)}$  [27, Chapter 4]. This matrix can be conveniently partitioned as

$$\mathbf{Z}_H = \begin{bmatrix} \mathbf{Z}_{TT} & \mathbf{Z}_{TR} \\ \mathbf{Z}_{RT} & \mathbf{Z}_{RR} \end{bmatrix}, \quad (2)$$

where  $\mathbf{Z}_{TT} \in \mathbb{C}^{N_T \times N_T}$  and  $\mathbf{Z}_{RR} \in \mathbb{C}^{N_R \times N_R}$  are the impedance matrices at the transmitting and receiving antenna arrays. The off-diagonal entries of  $\mathbf{Z}_{TT}$  and  $\mathbf{Z}_{RR}$  are the antenna mutual coupling effects, and the diagonal entries of  $\mathbf{Z}_{TT}$  and  $\mathbf{Z}_{RR}$  are the antenna self-impedances. Besides,  $\mathbf{Z}_{RT}$  is the transmission impedance matrix from the transmitter to the receiver, and  $\mathbf{Z}_{TR} = \mathbf{Z}_{RT}^T$  for the reciprocity of the channel. Following the definition of impedance matrix [27, Chapter 4], we have

$$\begin{bmatrix} \mathbf{x} \\ \mathbf{z} \end{bmatrix} = \begin{bmatrix} \mathbf{Z}_{TT} & \mathbf{Z}_{TR} \\ \mathbf{Z}_{RT} & \mathbf{Z}_{RR} \end{bmatrix} \begin{bmatrix} \mathbf{i}_x \\ \mathbf{i}_z \end{bmatrix}, \quad (3)$$

where the directions of the currents are shown in Fig. 1. At the transmitter,  $\mathbf{x}$  and  $\mathbf{i}_x$  are related to the source vector  $\mathbf{s}$  by

$$\mathbf{x} = \mathbf{s} - Z_0 \mathbf{i}_x, \quad (4)$$

which is obtained by applying Ohm's law at all the transmitting antennas, and where the minus sign is in agreement with

the current directions in Fig. 1. At the receiver,  $\mathbf{z}$  and  $\mathbf{i}_z$  are related by

$$\mathbf{z} = -Z_0 \mathbf{i}_z, \quad (5)$$

following Ohm's law.

The channel  $\mathbf{H}$  can now be derived by solving the system of the three equations (3), (4), and (5), which is compactly written as

$$\begin{cases} \mathbf{v} = \mathbf{Z}_H \mathbf{i}, \\ \mathbf{v} = \bar{\mathbf{s}} - Z_0 \mathbf{i}, \end{cases} \quad (6)$$

where we introduced  $\mathbf{v} \in \mathbb{C}^{(N_T + N_R) \times 1}$ ,  $\mathbf{i} \in \mathbb{C}^{(N_T + N_R) \times 1}$ , and  $\bar{\mathbf{s}} \in \mathbb{C}^{(N_T + N_R) \times 1}$  as

$$\mathbf{v} = \begin{bmatrix} \mathbf{x} \\ \mathbf{z} \end{bmatrix}, \quad \mathbf{i} = \begin{bmatrix} \mathbf{i}_x \\ \mathbf{i}_z \end{bmatrix}, \quad \bar{\mathbf{s}} = \begin{bmatrix} \mathbf{s} \\ \mathbf{0} \end{bmatrix}. \quad (7)$$

System (6) gives  $\mathbf{v} = \mathbf{Z}_H (\mathbf{Z}_H + Z_0 \mathbf{I})^{-1} \bar{\mathbf{s}}$ . Thus, by introducing  $\mathbf{A} \in \mathbb{C}^{(N_T + N_R) \times (N_T + N_R)}$  as

$$\mathbf{A} = \mathbf{Z}_H (\mathbf{Z}_H + Z_0 \mathbf{I})^{-1}, \quad (8)$$

partitioned as

$$\mathbf{A} = \begin{bmatrix} \mathbf{A}_{11} & \mathbf{A}_{12} \\ \mathbf{A}_{21} & \mathbf{A}_{22} \end{bmatrix}, \quad (9)$$

with  $\mathbf{A}_{11} \in \mathbb{C}^{N_T \times N_T}$ ,  $\mathbf{A}_{22} \in \mathbb{C}^{N_R \times N_R}$ , we have  $\mathbf{z} = \mathbf{A}_{21} \mathbf{s}$ . By comparing the relationship  $\mathbf{z} = \mathbf{A}_{21} \mathbf{s}$  with  $\mathbf{z} = \mathbf{H} \mathbf{s}$ , we notice that  $\mathbf{H} = \mathbf{A}_{21}$ , which is derived in the following.

To simplify the derivation, we consider the unilateral approximation [18], i.e., we assume that the electrical properties at the transmitter are independent of the electrical properties at the receiver. This assumption accurately reflects what happens in common wireless systems and allows us to neglect the feedback channel by setting it as  $\mathbf{Z}_{TR} = \mathbf{0}$ . Expanding  $\mathbf{Z}_H$  in (8), we can therefore write  $\mathbf{A}$  as

$$\mathbf{A} = \begin{bmatrix} \mathbf{Z}_{TT} & \mathbf{0} \\ \mathbf{Z}_{RT} & \mathbf{Z}_{RR} \end{bmatrix} \begin{bmatrix} \mathbf{Z}_{TT} + Z_0 \mathbf{I} & \mathbf{0} \\ \mathbf{Z}_{RT} & \mathbf{Z}_{RR} + Z_0 \mathbf{I} \end{bmatrix}^{-1}. \quad (10)$$

By carrying out the matrix inverse in (10) (note that the matrix to be inverted is a lower triangular  $2 \times 2$  block matrix) and the matrix product, we obtain

$$\mathbf{H} = \mathbf{A}_{21} = Z_0 (\mathbf{Z}_{RR} + Z_0 \mathbf{I})^{-1} \mathbf{Z}_{RT} (\mathbf{Z}_{TT} + Z_0 \mathbf{I})^{-1}, \quad (11)$$

giving our desired wireless channel matrix, in agreement with [17, Section II].

#### B. Model With No Mutual Coupling

The obtained channel model can be simplified by assuming that all antennas are perfectly matched to  $Z_0$  and neglecting the mutual coupling effects, which is realistic when the antenna spacing is at least half-wavelength. First, when all antennas at the transmitter and receiver are perfectly matched to  $Z_0$ , namely their self-impedances are all  $Z_0$ , the diagonal entries of  $\mathbf{Z}_{TT}$  and  $\mathbf{Z}_{RR}$  are all equal to  $Z_0$ . Second, with no mutual coupling, the off-diagonal entries of  $\mathbf{Z}_{TT}$  and  $\mathbf{Z}_{RR}$  are all zero. Therefore, under these two assumptions, we have  $\mathbf{Z}_{TT} = Z_0 \mathbf{I}$  and  $\mathbf{Z}_{RR} = Z_0 \mathbf{I}$ , which simplify the channel model in (11) as  $\mathbf{H} = \mathbf{Z}_{RT} / (4Z_0)$ , purely depending on the transmission impedance matrix  $\mathbf{Z}_{RT}$ .

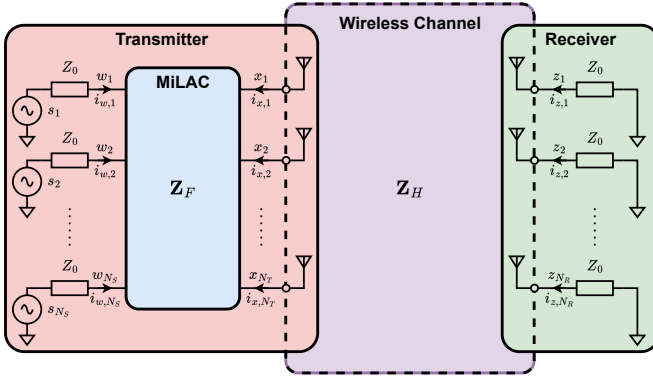


Fig. 2. Model of a MIMO system with MiLAC at the transmitter.

### III. MODELING A MIMO SYSTEM WITH MiLAC AT THE TRANSMITTER

We have analyzed a conventional digital MIMO system with multiport network analysis. In this section, we show how to apply the same tools to analyze a MIMO system where the transmitter is equipped with a MiLAC, as shown in Fig. 2.

At the transmitter, we denote the voltages at the generators as  $\mathbf{s} \in \mathbb{C}^{N_S \times 1}$ , where  $N_S$  is the number of RF chains, the voltages and currents at the input of the MiLAC as  $\mathbf{w} \in \mathbb{C}^{N_S \times 1}$  and  $\mathbf{i}_w \in \mathbb{C}^{N_S \times 1}$ , and the voltages and currents at the transmitting antennas as  $\mathbf{x} \in \mathbb{C}^{N_T \times 1}$  and  $\mathbf{i}_x \in \mathbb{C}^{N_T \times 1}$ , where  $N_T$  is the number of transmitting antennas. At the receiver, we denote the voltages and currents as  $\mathbf{z} \in \mathbb{C}^{N_R \times 1}$  and  $\mathbf{i}_z \in \mathbb{C}^{N_R \times 1}$ , where  $N_R$  is the number of receiving antennas (which is the same as the number of RF chains at the receiver since it operates digital beamforming). The received signal  $\mathbf{z}$  is given as a function of the transmitted signal  $\mathbf{s}$  by

$$\mathbf{z} = \mathbf{H}\mathbf{F}\mathbf{s}, \quad (12)$$

where  $\mathbf{H} \in \mathbb{C}^{N_R \times N_T}$  is the wireless channel matrix and  $\mathbf{F} \in \mathbb{C}^{N_T \times N_S}$  is the precoding matrix implemented by the MiLAC. In the following, we derive accurate expressions for  $\mathbf{H}$  and  $\mathbf{F}$  in the presence of mutual coupling at both the transmitter and receiver.

#### A. Model With Mutual Coupling

As it was done for the digital MIMO system in Section II, we first derive the relationships between the signals at the wireless channel, the transmitter, and the receiver, and then consider them jointly to derive the system model. The wireless channel can be seen as a  $(N_T + N_R)$ -port network with impedance matrix  $\mathbf{Z}_H \in \mathbb{C}^{(N_T + N_R) \times (N_T + N_R)}$ , partitioned as in (2). Therefore, according to the definition of impedance matrix [27, Chapter 4], the voltages and currents at the transmitting antennas and at the receiver are related by

$$\begin{bmatrix} \mathbf{x} \\ \mathbf{z} \end{bmatrix} = \begin{bmatrix} \mathbf{Z}_{TT} & \mathbf{Z}_{TR} \\ \mathbf{Z}_{RT} & \mathbf{Z}_{RR} \end{bmatrix} \begin{bmatrix} -\mathbf{i}_x \\ \mathbf{i}_z \end{bmatrix}, \quad (13)$$

where the directions of the currents  $\mathbf{i}_x$  and  $\mathbf{i}_z$  are illustrated in Fig. 2. At the transmitter,  $\mathbf{w}$  and  $\mathbf{i}_w$  are related to the source vector  $\mathbf{s}$  by

$$\mathbf{w} = \mathbf{s} - Z_0 \mathbf{i}_w, \quad (14)$$

following Ohm's law. In addition, introducing the impedance matrix of the MiLAC as  $\mathbf{Z}_F \in \mathbb{C}^{(N_S + N_T) \times (N_S + N_T)}$ , partitioned as

$$\mathbf{Z}_F = \begin{bmatrix} \mathbf{Z}_{F,11} & \mathbf{Z}_{F,12} \\ \mathbf{Z}_{F,21} & \mathbf{Z}_{F,22} \end{bmatrix}, \quad (15)$$

where  $\mathbf{Z}_{F,11} \in \mathbb{C}^{N_S \times N_S}$  and  $\mathbf{Z}_{F,22} \in \mathbb{C}^{N_T \times N_T}$ , we have

$$\begin{bmatrix} \mathbf{w} \\ \mathbf{x} \end{bmatrix} = \begin{bmatrix} \mathbf{Z}_{F,11} & \mathbf{Z}_{F,12} \\ \mathbf{Z}_{F,21} & \mathbf{Z}_{F,22} \end{bmatrix} \begin{bmatrix} \mathbf{i}_w \\ \mathbf{i}_x \end{bmatrix}, \quad (16)$$

by the definition of impedance matrix [27, Chapter 4]. Finally, at the receiver, we have

$$\mathbf{z} = -Z_0 \mathbf{i}_z, \quad (17)$$

as for the conventional MIMO system in Section II.

To derive the channel  $\mathbf{H}$  and the precoder  $\mathbf{F}$ , we need now to solve the system of the four equations (13), (14), (16), and (17). Considering the unilateral approximation [18], i.e.,  $\mathbf{Z}_{TR} = \mathbf{0}$ , this system can be compactly written as

$$\begin{cases} \mathbf{v} = \mathbf{Z}\mathbf{i}, \\ \mathbf{v} = \bar{\mathbf{s}} - \bar{\mathbf{Z}}\mathbf{i}, \end{cases} \quad (18)$$

where we introduced  $\mathbf{v} \in \mathbb{C}^{(N_S + N_T + N_R) \times 1}$ ,  $\mathbf{i} \in \mathbb{C}^{(N_S + N_T + N_R) \times 1}$ ,  $\mathbf{Z} \in \mathbb{C}^{(N_S + N_T + N_R) \times (N_S + N_T + N_R)}$ ,  $\bar{\mathbf{s}} \in \mathbb{C}^{(N_S + N_T + N_R) \times 1}$ , and  $\bar{\mathbf{Z}} \in \mathbb{C}^{(N_S + N_T + N_R) \times (N_S + N_T + N_R)}$  as

$$\mathbf{v} = \begin{bmatrix} \mathbf{w} \\ \mathbf{x} \\ \mathbf{z} \end{bmatrix}, \mathbf{i} = \begin{bmatrix} \mathbf{i}_w \\ \mathbf{i}_x \\ \mathbf{i}_z \end{bmatrix}, \mathbf{Z} = \begin{bmatrix} \mathbf{Z}_{F,11} & \mathbf{Z}_{F,12} & \mathbf{0} \\ \mathbf{Z}_{F,21} & \mathbf{Z}_{F,22} & \mathbf{0} \\ \mathbf{0} & -\mathbf{Z}_{RT} & \mathbf{Z}_{RR} \end{bmatrix}, \quad (19)$$

$$\bar{\mathbf{s}} = \begin{bmatrix} \mathbf{s} \\ \mathbf{0} \\ \mathbf{0} \end{bmatrix}, \bar{\mathbf{Z}} = \begin{bmatrix} Z_0 \mathbf{I} & \mathbf{0} & \mathbf{0} \\ \mathbf{0} & \mathbf{Z}_{TT} & \mathbf{0} \\ \mathbf{0} & \mathbf{0} & Z_0 \mathbf{I} \end{bmatrix}. \quad (20)$$

System (18) gives  $\mathbf{v} = \mathbf{Z}(\mathbf{Z} + \bar{\mathbf{Z}})^{-1} \bar{\mathbf{s}}$ . Thus, by introducing  $\mathbf{A} \in \mathbb{C}^{(N_S + N_T + N_R) \times (N_S + N_T + N_R)}$  as

$$\mathbf{A} = \mathbf{Z}(\mathbf{Z} + \bar{\mathbf{Z}})^{-1}, \quad (21)$$

partitioned as

$$\mathbf{A} = \begin{bmatrix} \mathbf{A}_{11} & \mathbf{A}_{12} & \mathbf{A}_{13} \\ \mathbf{A}_{21} & \mathbf{A}_{22} & \mathbf{A}_{23} \\ \mathbf{A}_{31} & \mathbf{A}_{32} & \mathbf{A}_{33} \end{bmatrix}, \quad (22)$$

with  $\mathbf{A}_{11} \in \mathbb{C}^{N_S \times N_S}$ ,  $\mathbf{A}_{22} \in \mathbb{C}^{N_T \times N_T}$ , and  $\mathbf{A}_{33} \in \mathbb{C}^{N_R \times N_R}$ , we have  $\mathbf{z} = \mathbf{A}_{31}\mathbf{s}$ . By comparing the relationship  $\mathbf{z} = \mathbf{A}_{31}\mathbf{s}$  with  $\mathbf{z} = \mathbf{H}\mathbf{F}\mathbf{s}$ , we notice that  $\mathbf{H}\mathbf{F} = \mathbf{A}_{31}$ .

To obtain the expression of  $\mathbf{A}_{31}$ , we introduce  $\tilde{\mathbf{Z}}_{RT} \in \mathbb{C}^{N_R \times (N_S + N_T)}$  and  $\tilde{\mathbf{Z}}_{TT} \in \mathbb{C}^{(N_S + N_T) \times (N_S + N_T)}$  as

$$\tilde{\mathbf{Z}}_{RT} = \begin{bmatrix} \mathbf{0} & \mathbf{Z}_{RT} \end{bmatrix}, \tilde{\mathbf{Z}}_{TT} = \begin{bmatrix} Z_0 \mathbf{I} & \mathbf{0} \\ \mathbf{0} & \mathbf{Z}_{TT} \end{bmatrix}, \quad (23)$$

such that  $\mathbf{A} = \mathbf{Z}(\mathbf{Z} + \bar{\mathbf{Z}})^{-1}$  can be rewritten as

$$\mathbf{A} = \begin{bmatrix} \mathbf{Z}_F & \mathbf{0} \\ -\tilde{\mathbf{Z}}_{RT} & \mathbf{Z}_{RR} \end{bmatrix} \begin{bmatrix} \mathbf{Z}_F + \tilde{\mathbf{Z}}_{TT} & \mathbf{0} \\ -\tilde{\mathbf{Z}}_{RT} & \mathbf{Z}_{RR} + Z_0 \mathbf{I} \end{bmatrix}^{-1}. \quad (24)$$

By carrying out the matrix inverse in (24) (note that the matrix to be inverted is a lower triangular  $2 \times 2$  block matrix) and the matrix product, we obtain

$$\begin{aligned} [\mathbf{A}_{31} \quad \mathbf{A}_{32}] = \\ -Z_0 (\mathbf{Z}_{RR} + Z_0 \mathbf{I})^{-1} \tilde{\mathbf{Z}}_{RT} (\mathbf{Z}_F + \tilde{\mathbf{Z}}_{TT})^{-1}. \end{aligned} \quad (25)$$

By substituting (23) into (25), and carrying out the necessary computations, we obtain

$$\begin{aligned} \mathbf{A}_{31} = Z_0 (\mathbf{Z}_{RR} + Z_0 \mathbf{I})^{-1} \mathbf{Z}_{RT} \mathbf{Z}_{TT}^{-1} \\ \times \left[ \left( \frac{\mathbf{Y}_F}{Y_0} + \begin{bmatrix} \mathbf{I} & \mathbf{0} \\ \mathbf{0} & \frac{\mathbf{Z}_{TT}^{-1}}{Y_0} \end{bmatrix} \right)^{-1} \right]_{N_S+(1:N_T), 1:N_S}, \end{aligned} \quad (26)$$

where we introduced  $\mathbf{Y}_F = \mathbf{Z}_F^{-1}$  as the admittance matrix of the MiLAC and  $Y_0 = Z_0^{-1}$ . Since  $\mathbf{H}\mathbf{F} = \mathbf{A}_{31}$ , we identify the channel matrix  $\mathbf{H}$  and the MiLAC precoding matrix  $\mathbf{F}$  as

$$\mathbf{H} = Z_0 (\mathbf{Z}_{RR} + Z_0 \mathbf{I})^{-1} \mathbf{Z}_{RT} \mathbf{Z}_{TT}^{-1}, \quad (27)$$

and

$$\mathbf{F} = \left[ \left( \frac{\mathbf{Y}_F}{Y_0} + \begin{bmatrix} \mathbf{I} & \mathbf{0} \\ \mathbf{0} & \frac{\mathbf{Z}_{TT}^{-1}}{Y_0} \end{bmatrix} \right)^{-1} \right]_{N_S+(1:N_T), 1:N_S}, \quad (28)$$

showing that  $\mathbf{F}$  depends not only on the admittance matrix of the MiLAC  $\mathbf{Y}_F$ , but also on the mutual coupling matrix at the transmitter  $\mathbf{Z}_{TT}$ .

Note that by plugging (23) into (25), we can also obtain an alternative expression of the end-to-end channel  $\mathbf{A}_{31}$  following different steps, namely

$$\mathbf{A}_{31} = Z_0 (\mathbf{Z}_{RR} + Z_0 \mathbf{I})^{-1} \mathbf{Z}_{RT} \mathbf{J}_T^T (\mathbf{Z}_T + Z_0 \mathbf{I})^{-1}, \quad (29)$$

where we introduced  $\mathbf{Z}_T \in \mathbb{C}^{N_S \times N_S}$  and  $\mathbf{J}_T \in \mathbb{C}^{N_S \times N_T}$  as

$$\mathbf{Z}_T = \mathbf{Z}_{F,11} - \mathbf{J}_T \mathbf{Z}_{F,21}, \quad (30)$$

$$\mathbf{J}_T = \mathbf{Z}_{F,12} (\mathbf{Z}_{F,22} + \mathbf{Z}_{TT})^{-1}. \quad (31)$$

This expression, based on the MiLAC impedance matrix  $\mathbf{Z}_F$  rather than the MiLAC admittance matrix  $\mathbf{Y}_F$ , has been used to study the impact of matching networks on MIMO channels [18, Section II]. Therefore, a MiLAC has the same impact on the channel expression as a matching network. Nevertheless, while a matching network is fixed and it is designed to maximize the power flow from the generators to the antennas in the presence of mutual coupling, a MiLAC is reconfigurable and can perform beamforming depending on the channel realization. A MiLAC alleviates the baseband processing needs at the cost of a reconfigurable microwave network. In terms of representation, it is convenient to represent the effect of a MiLAC with its admittance matrix as in (28), since it is closely related to its tunable components, as specified in [10].

### B. Model With No Mutual Coupling

Assuming perfect matching and no mutual coupling at both the transmitter and receiver, the expressions of the channel matrix  $\mathbf{H}$  and precoding matrix  $\mathbf{F}$  can be significantly simplified. In particular, as a consequence of perfect matching

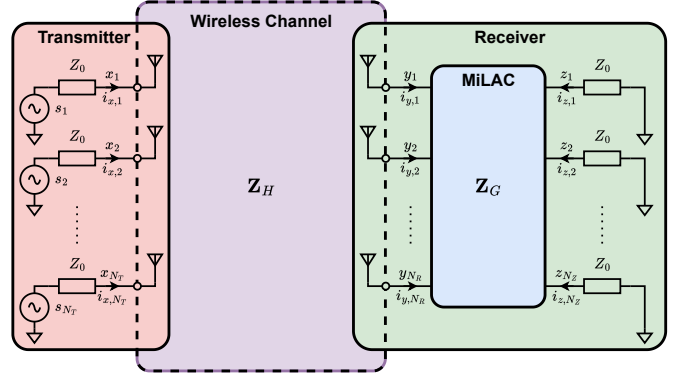


Fig. 3. Model of a MIMO system with MiLAC at the receiver.

and with negligible mutual coupling, we have  $\mathbf{Z}_T = Z_0 \mathbf{I}$  and  $\mathbf{Z}_R = Z_0 \mathbf{I}$ . By substituting  $\mathbf{Z}_T = Z_0 \mathbf{I}$  and  $\mathbf{Z}_R = Z_0 \mathbf{I}$  into (27) and (28), we obtain  $\mathbf{H} = \mathbf{Z}_{RT} / (2Z_0)$  and

$$\mathbf{F} = \left[ \left( \frac{\mathbf{Y}_F}{Y_0} + \mathbf{I} \right)^{-1} \right]_{N_S+(1:N_T), 1:N_S}, \quad (32)$$

in agreement with previous literature on MiLAC [10], [11].

## IV. MODELING A MIMO SYSTEM WITH MiLAC AT THE RECEIVER

We have analyzed a MIMO system with MiLAC at the transmitter, and derived the expressions of the channel and precoding matrix with and without mutual coupling effects. In this section, we carry out the same analysis for a MIMO system where the receiver is equipped with a MiLAC, as shown in Fig. 3.

At the transmitter, we denote the voltages at the voltage generators as  $\mathbf{s} \in \mathbb{C}^{N_T \times 1}$ , and the voltages and currents at the transmitting antennas as  $\mathbf{x} \in \mathbb{C}^{N_T \times 1}$  and  $\mathbf{i}_x \in \mathbb{C}^{N_T \times 1}$ , where  $N_T$  is the number of antennas. At the receiver, we denote the voltages and currents at the receiving antennas as  $\mathbf{y} \in \mathbb{C}^{N_R \times 1}$  and  $\mathbf{i}_y \in \mathbb{C}^{N_R \times 1}$ , where  $N_R$  is the number of antennas, and the voltages and currents at the receiving RF chains as  $\mathbf{z} \in \mathbb{C}^{N_Z \times 1}$  and  $\mathbf{i}_z \in \mathbb{C}^{N_Z \times 1}$ , where  $N_Z$  the number of receiving RF chains. The received signal  $\mathbf{z}$  is given as a function of the transmitted signal  $\mathbf{s}$  by

$$\mathbf{z} = \mathbf{G}\mathbf{H}\mathbf{s}, \quad (33)$$

where  $\mathbf{G} \in \mathbb{C}^{N_Z \times N_R}$  is the combining matrix implemented by the MiLAC and  $\mathbf{H} \in \mathbb{C}^{N_R \times N_T}$  is the wireless channel matrix. Our goal is to derive accurate expressions for  $\mathbf{G}$  and  $\mathbf{H}$  in the presence of mutual coupling at both the transmitter and receiver.

### A. Model With Mutual Coupling

We begin by deriving the relationships between the signals at the wireless channel, the transmitter, and the receiver, and then solve a system of equations involving all these relationships. We represent the wireless channel as a  $(N_T + N_R)$ -port network with impedance matrix  $\mathbf{Z}_H \in \mathbb{C}^{(N_T+N_R) \times (N_T+N_R)}$ , partitioned as in (2). Following the definition of impedance

matrix, the voltages and currents at the transmitting and receiving antennas are related by

$$\begin{bmatrix} \mathbf{x} \\ \mathbf{y} \end{bmatrix} = \begin{bmatrix} \mathbf{Z}_{TT} & \mathbf{Z}_{TR} \\ \mathbf{Z}_{RT} & \mathbf{Z}_{RR} \end{bmatrix} \begin{bmatrix} \mathbf{i}_x \\ -\mathbf{i}_y \end{bmatrix}, \quad (34)$$

where the direction of the currents is shown in Fig. 3. At the transmitter, we have

$$\mathbf{x} = \mathbf{s} - Z_0 \mathbf{i}_x, \quad (35)$$

as for the conventional MIMO system in Section II. At the receiver, we introduce the impedance matrix of the MiLAC as  $\mathbf{Z}_G \in \mathbb{C}^{(N_R+N_Z) \times (N_R+N_Z)}$ , partitioned as

$$\mathbf{Z}_G = \begin{bmatrix} \mathbf{Z}_{G,11} & \mathbf{Z}_{G,12} \\ \mathbf{Z}_{G,21} & \mathbf{Z}_{G,22} \end{bmatrix}, \quad (36)$$

where  $\mathbf{Z}_{G,11} \in \mathbb{C}^{N_R \times N_R}$  and  $\mathbf{Z}_{G,22} \in \mathbb{C}^{N_Z \times N_Z}$ , which gives

$$\begin{bmatrix} \mathbf{y} \\ \mathbf{z} \end{bmatrix} = \begin{bmatrix} \mathbf{Z}_{G,11} & \mathbf{Z}_{G,12} \\ \mathbf{Z}_{G,21} & \mathbf{Z}_{G,22} \end{bmatrix} \begin{bmatrix} \mathbf{i}_y \\ \mathbf{i}_z \end{bmatrix}, \quad (37)$$

by the definition of impedance matrix [27, Chapter 4]. In addition,  $\mathbf{z}$  and  $\mathbf{i}_z$  are related by

$$\mathbf{z} = -Z_0 \mathbf{i}_z, \quad (38)$$

by Ohm's law.

To derive the channel  $\mathbf{H}$  and the combiner  $\mathbf{G}$ , we solve the system of the four equations (34), (35), (37), and (38). With the unilateral approximation [18], i.e.,  $\mathbf{Z}_{TR} = \mathbf{0}$ , it is possible to show that a procedure similar to the one used in Section III yields

$$\mathbf{GH} = \left[ \left( \frac{\mathbf{Y}_G}{Y_0} + \begin{bmatrix} \mathbf{Z}_{RR}^{-1} & \mathbf{0} \\ \mathbf{0} & \mathbf{I} \end{bmatrix} \right)^{-1} \right]_{N_R+(1:N_Z),1:N_R} \times Z_0 \mathbf{Z}_{RR}^{-1} \mathbf{Z}_{RT} (\mathbf{Z}_{TT} + Z_0 \mathbf{I})^{-1}, \quad (39)$$

where we introduced  $\mathbf{Y}_G = \mathbf{Z}_G^{-1}$  as the admittance matrix of the MiLAC. Therefore, we identify the channel  $\mathbf{H}$  and the combiner  $\mathbf{G}$  as

$$\mathbf{H} = Z_0 \mathbf{Z}_{RR}^{-1} \mathbf{Z}_{RT} (\mathbf{Z}_{TT} + Z_0 \mathbf{I})^{-1}, \quad (40)$$

and

$$\mathbf{G} = \left[ \left( \frac{\mathbf{Y}_G}{Y_0} + \begin{bmatrix} \mathbf{Z}_{RR}^{-1} & \mathbf{0} \\ \mathbf{0} & \mathbf{I} \end{bmatrix} \right)^{-1} \right]_{N_R+(1:N_Z),1:N_R}, \quad (41)$$

showing that the combiner  $\mathbf{G}$  depends on the admittance matrix of the MiLAC  $\mathbf{Y}_G$  and also on the mutual coupling matrix at the receiver  $\mathbf{Z}_{RR}$ .

It is worthwhile to compare the channel expressions obtained for MiLAC at the transmitter and receiver given by (27) and (40), respectively. To distinguish between them, we denote the channels in (27) and (40) as  $\mathbf{H}_{Tx}$  and  $\mathbf{H}_{Rx}$ , respectively. Since  $\mathbf{H}_{Tx}$  and  $\mathbf{H}_{Rx}$  are the channel expressions of the same wireless system where the roles of the transmitter and receiver are swapped, it should hold  $\mathbf{H}_{Tx}^T = \mathbf{H}_{Rx}$  in the case of a reciprocal channel, which is demonstrated in the following. By taking the transpose of  $\mathbf{H}_{Tx}$  in (27), we obtain  $\mathbf{H}_{Tx}^T = Z_0 (\mathbf{Z}_{TT}^{-1})^T \mathbf{Z}_{RT}^T ((\mathbf{Z}_{RR} + Z_0 \mathbf{I})^{-1})^T$ , which can

be rewritten as  $\mathbf{H}_{Tx}^T = Z_0 \mathbf{Z}_{TT}^{-1} \mathbf{Z}_{TR} (\mathbf{Z}_{RR} + Z_0 \mathbf{I})^{-1}$  since  $\mathbf{Z}_{TT}^T = \mathbf{Z}_{TT}^{-1}$ ,  $\mathbf{Z}_{TR} = \mathbf{Z}_{RT}^T$ , and  $\mathbf{Z}_{RR} = \mathbf{Z}_{RR}^T$  in the case of a reciprocal channel. By swapping the roles of the transmitter and receiver, i.e., by substituting  $\mathbf{Z}_{TT}$ ,  $\mathbf{Z}_{TR}$ , and  $\mathbf{Z}_{RR}$  with  $\mathbf{Z}_{RR}$ ,  $\mathbf{Z}_{RT}$ , and  $\mathbf{Z}_{TT}$ , respectively, we have that the expression of  $\mathbf{H}_{Tx}^T$  coincides with (40), showing that  $\mathbf{H}_{Tx}^T = \mathbf{H}_{Rx}$ .

By solving the system of equations (34), (35), (37), and (38) with alternative derivations, we can also obtain a different but equivalent expression of the end-to-end channel  $\mathbf{GH}$ , i.e.,

$$\mathbf{GH} = Z_0 (\mathbf{Z}_R + Z_0 \mathbf{I})^{-1} \mathbf{J}_R \mathbf{Z}_{RT} (\mathbf{Z}_{TT} + Z_0 \mathbf{I})^{-1}, \quad (42)$$

where  $\mathbf{Z}_R \in \mathbb{C}^{N_Z \times N_Z}$  and  $\mathbf{J}_R \in \mathbb{C}^{N_Z \times N_R}$  are

$$\mathbf{Z}_R = \mathbf{Z}_{G,22} - \mathbf{J}_R \mathbf{Z}_{G,12}, \quad (43)$$

$$\mathbf{J}_R = \mathbf{Z}_{G,21} (\mathbf{Z}_{G,11} + \mathbf{Z}_{RR})^{-1}. \quad (44)$$

This expression depends on the MiLAC impedance matrix  $\mathbf{Z}_G$  rather than the admittance matrix  $\mathbf{Y}_G$ , and has been used to study the impact of matching networks in MIMO channels [18, Section II]. Therefore, a MiLAC at the receiver has the same impact on the channel expression as a matching network. In terms of representation, it is convenient to represent the effect of a MiLAC with its admittance matrix as in (41), since it is closely related to its tunable components [10].

### B. Model With No Mutual Coupling

We now assume all antennas to be perfectly matched to  $Z_0$  and that the mutual coupling effects are negligible, which jointly give  $\mathbf{Z}_T = Z_0 \mathbf{I}$  and  $\mathbf{Z}_R = Z_0 \mathbf{I}$ . By substituting  $\mathbf{Z}_T = Z_0 \mathbf{I}$  and  $\mathbf{Z}_R = Z_0 \mathbf{I}$  into (40) and (41), we obtain that the channel matrix is given by  $\mathbf{H} = \mathbf{Z}_{RT} / (2Z_0)$  as in Section III, while the combining matrix of the MiLAC boils down to

$$\mathbf{G} = \left[ \left( \frac{\mathbf{Y}_G}{Y_0} + \mathbf{I} \right)^{-1} \right]_{N_R+(1:N_Z),1:N_R}, \quad (45)$$

which agrees with prior works on MiLAC [10], [11].

## V. MODELING A MIMO SYSTEM WITH MiLAC AT BOTH THE TRANSMITTER AND RECEIVER

In this section, we analyze a MIMO system where both the transmitter and receiver have a MiLAC, as shown in Fig. 4.

At the transmitter, we denote the source voltages as  $\mathbf{s} \in \mathbb{C}^{N_S \times 1}$ , where  $N_S$  is the number of RF chains, the voltages and currents at the input of the MiLAC as  $\mathbf{w} \in \mathbb{C}^{N_S \times 1}$  and  $\mathbf{i}_w \in \mathbb{C}^{N_S \times 1}$ , and the voltages and currents at the transmitting antennas as  $\mathbf{x} \in \mathbb{C}^{N_T \times 1}$  and  $\mathbf{i}_x \in \mathbb{C}^{N_T \times 1}$ , where  $N_T$  is the number of antennas. At the receiver, we denote the voltages and currents at the receiving antennas as  $\mathbf{y} \in \mathbb{C}^{N_R \times 1}$  and  $\mathbf{i}_y \in \mathbb{C}^{N_R \times 1}$ , where  $N_R$  is the number of antennas, and the voltages and currents at the output of the MiLAC as  $\mathbf{z} \in \mathbb{C}^{N_Z \times 1}$  and  $\mathbf{i}_z \in \mathbb{C}^{N_Z \times 1}$ , where  $N_Z$  the number of RF chains. The received signal  $\mathbf{z}$  is related to the transmitted signal  $\mathbf{s}$  by

$$\mathbf{z} = \mathbf{GHF}, \quad (46)$$

where  $\mathbf{G} \in \mathbb{C}^{N_Z \times N_R}$  is the combining matrix implemented by the receiver-side MiLAC,  $\mathbf{H} \in \mathbb{C}^{N_R \times N_T}$  is the wireless channel, and  $\mathbf{F} \in \mathbb{C}^{N_T \times N_S}$  is the precoding matrix implemented

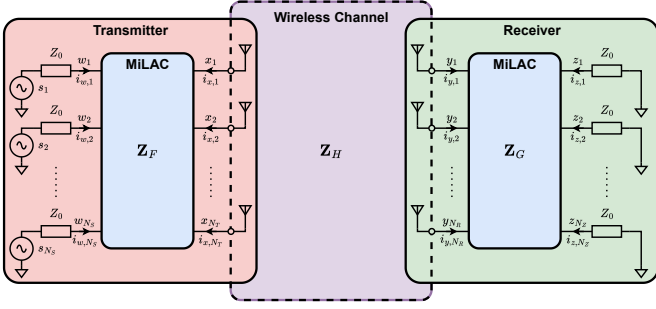


Fig. 4. Model of a MIMO system with MiLAC at both the transmitter and receiver.

by the transmitter-side MiLAC. Our goal is to derive accurate expressions for  $\mathbf{G}$ ,  $\mathbf{H}$ , and  $\mathbf{F}$  that include the effects of mutual coupling between antennas.

### A. Model With Mutual Coupling

As done in the previous sections, we first derive the relationships between the signals at the wireless channel, the transmitter, and the receiver, and then solve the system of equations including all of them to obtain  $\mathbf{G}$ ,  $\mathbf{H}$ , and  $\mathbf{F}$ . The wireless channel is modeled as a  $(N_T + N_R)$ -port network with impedance matrix  $\mathbf{Z}_H \in \mathbb{C}^{(N_T + N_R) \times (N_T + N_R)}$ , partitioned as in (2). Therefore, we have

$$\begin{bmatrix} \mathbf{x} \\ \mathbf{y} \end{bmatrix} = \begin{bmatrix} \mathbf{Z}_{TT} & \mathbf{Z}_{TR} \\ \mathbf{Z}_{RT} & \mathbf{Z}_{RR} \end{bmatrix} \begin{bmatrix} -\mathbf{i}_x \\ -\mathbf{i}_y \end{bmatrix}, \quad (47)$$

where the currents are defined with directions as represented in Fig. 4. At the transmitter,  $\mathbf{w}$  and  $\mathbf{i}_w$  are related to the source vector  $\mathbf{s}$  as

$$\mathbf{w} = \mathbf{s} - Z_0 \mathbf{i}_w, \quad (48)$$

by Ohm's law, and, introducing the impedance matrix of the MiLAC as  $\mathbf{Z}_F$ , the voltages and currents at the MiLAC ports are related by (16). At the receiver, we similarly introduce the impedance matrix of the MiLAC as  $\mathbf{Z}_G$  such that the relationship between voltages and currents in (37) holds. In addition,  $\mathbf{z}$  and  $\mathbf{i}_z$  are also related by

$$\mathbf{z} = -Z_0 \mathbf{i}_z, \quad (49)$$

because of Ohm's law.

The matrices  $\mathbf{G}$ ,  $\mathbf{H}$ , and  $\mathbf{F}$  can be obtained by solving the system of the five equations (16), (37), (47), (48), and (49). With the unilateral approximation [18], i.e.,  $\mathbf{Z}_{TR} = \mathbf{0}$ , it is possible to show that a procedure similar to the one in the previous sections gives

$$\begin{aligned} \mathbf{GHF} &= \left[ \left( \frac{\mathbf{Y}_G}{Y_0} + \begin{bmatrix} \mathbf{Z}_{RR}^{-1} & \mathbf{0} \\ \mathbf{0} & \mathbf{I} \end{bmatrix} \right)^{-1} \right]_{N_R + (1:N_Z), 1:N_R} \\ &\quad \times Z_0 \mathbf{Z}_{RR}^{-1} \mathbf{Z}_{RT} \mathbf{Z}_{TT}^{-1} \\ &\quad \times \left[ \left( \frac{\mathbf{Y}_F}{Y_0} + \begin{bmatrix} \mathbf{I} & \mathbf{0} \\ \mathbf{0} & \mathbf{Z}_{TT}^{-1} \end{bmatrix} \right)^{-1} \right]_{N_S + (1:N_T), 1:N_S}, \quad (50) \end{aligned}$$

allowing us to identify the channel  $\mathbf{H}$  as

$$\mathbf{H} = Z_0 \mathbf{Z}_{RR}^{-1} \mathbf{Z}_{RT} \mathbf{Z}_{TT}^{-1}, \quad (51)$$

the precoder  $\mathbf{F}$  as in (28), and the combiner  $\mathbf{G}$  as in (41).

Departing from the system of five equations (16), (37), (47), (48), and (49), and executing different computations, we can reach an alternative expression of the end-to-end channel  $\mathbf{GHF}$  given by

$$\mathbf{GHF} = Z_0 (\mathbf{Z}_R + Z_0 \mathbf{I})^{-1} \mathbf{J}_R \mathbf{Z}_{RT} \mathbf{J}_T^T (\mathbf{Z}_T + Z_0 \mathbf{I})^{-1}, \quad (52)$$

where

$$\mathbf{Z}_T = \mathbf{Z}_{F,11} - \mathbf{J}_T \mathbf{Z}_{F,21}, \quad (53)$$

$$\mathbf{Z}_R = \mathbf{Z}_{G,22} - \mathbf{J}_R \mathbf{Z}_{G,12}, \quad (54)$$

$$\mathbf{J}_T = \mathbf{Z}_{F,12} (\mathbf{Z}_{F,22} + \mathbf{Z}_{TT})^{-1}, \quad (55)$$

$$\mathbf{J}_R = \mathbf{Z}_{G,21} (\mathbf{Z}_{G,11} + \mathbf{Z}_{RR})^{-1}. \quad (56)$$

This expression is in exact agreement with the end-to-end channel model of a digital MIMO system with a matching network at both the transmitter and receiver, as derived in [18, Section II]. However, MiLACs can be reconfigured on a per-channel realization basis, unlike matching networks, which are fixed, and it is therefore more convenient to characterize their effect through their admittance matrices rather than impedance matrices.

### B. Model With No Mutual Coupling

The derived system model can be simplified by assuming all antennas to be perfectly matched and neglecting the mutual coupling effects, yielding  $\mathbf{Z}_T = Z_0 \mathbf{I}$  and  $\mathbf{Z}_R = Z_0 \mathbf{I}$ . By substituting  $\mathbf{Z}_T = Z_0 \mathbf{I}$  and  $\mathbf{Z}_R = Z_0 \mathbf{I}$  in (51), the channel matrix simplifies as  $\mathbf{H} = \mathbf{Z}_{RT}/Z_0$ , while substituting  $\mathbf{Z}_T = Z_0 \mathbf{I}$  and  $\mathbf{Z}_R = Z_0 \mathbf{I}$  in the precoder  $\mathbf{F}$  and the combiner  $\mathbf{G}$  given by (28) and (41), they simplify as in (32) and (45), respectively.

## VI. PHYSICS-COMPLIANT OPTIMIZATION OF MiLAC

We have modeled MiLAC-aided MIMO systems accounting for the mutual coupling effects at the transmitter and receiver, and shown how the end-to-end system models vary depending on these effects. In this section, we focus on a MISO system with MiLAC at the transmitter and optimize the MiLAC in the presence of mutual coupling to maximize the received signal power.

Consider a MISO system with MiLAC at the transmitter, namely the same as in Section III with  $N_S = 1$  RF chain at the transmitter and  $N_R = 1$  antenna at the receiver, as shown in Fig. 5(a). Assuming the receiving antenna to be perfectly matched, i.e.,  $z_{RR} = Z_0$ , the received signal model derived in Section III boils down to

$$z = \mathbf{h} \mathbf{f} s, \quad (57)$$

where  $s$  is the transmitted symbol such that  $\mathbb{E}[|s|^2] = P_T$ , with  $P_T$  being the transmitted signal power. The wireless channel  $\mathbf{h} \in \mathbb{C}^{1 \times N_T}$  is

$$\mathbf{h} = \frac{1}{Z_0} \mathbf{z}_{RT} \mathbf{Y}_{TT}, \quad (58)$$

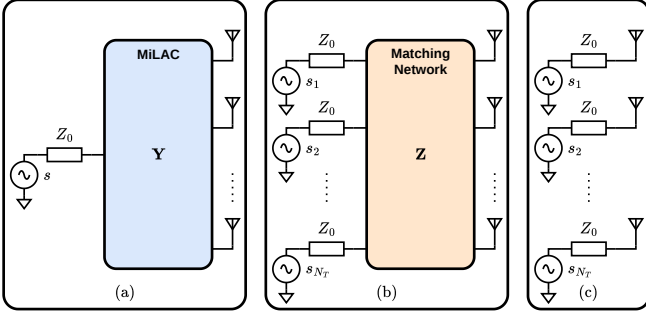


Fig. 5. Multi-antenna transmitter in a MISO system operating (a) MiLAC-aided beamforming, (b) digital beamforming with matching network, and (c) digital beamforming without matching network.

and the precoder implemented by the MiLAC  $\mathbf{f} \in \mathbb{C}^{N_T \times 1}$  is

$$\mathbf{f} = \left[ \left( \frac{\mathbf{Y}}{Y_0} + \begin{bmatrix} 1 & \mathbf{0} \\ \mathbf{0} & \mathbf{Y}_{TT} \end{bmatrix} \right)^{-1} \right]_{2:N_T+1,1}, \quad (59)$$

following (27) and (28), where we have denoted the admittance matrix of the MiLAC as  $\mathbf{Y}$  and introduced  $\mathbf{Y}_{TT} = \mathbf{Z}_{TT}^{-1}$  to simplify the notation. With perfect matching and no mutual coupling at the transmitter, we have  $\mathbf{Y}_{TT} = Y_0 \mathbf{I}$  and the expressions of  $\mathbf{h}$  and  $\mathbf{f}$  simplify to

$$\mathbf{h} = \frac{\mathbf{z}_{RT}}{2Z_0}, \quad \mathbf{f} = \left[ \left( \frac{\mathbf{Y}}{Y_0} + \mathbf{I} \right)^{-1} \right]_{2:N_T+1,1}. \quad (60)$$

For a MiLAC that is lossless and reciprocal, the admittance matrix  $\mathbf{Y}$  is purely imaginary and symmetric, i.e., it satisfies  $\mathbf{Y} = j\mathbf{B}$  and  $\mathbf{B} = \mathbf{B}^T$ , where  $\mathbf{B} \in \mathbb{R}^{(N_T+1) \times (N_T+1)}$  is the susceptance matrix of the MiLAC. Our goal is therefore to optimize the admittance matrix  $\mathbf{Y}$  subject to these constraints to maximize the received signal power  $P = P_T |\mathbf{h}\mathbf{f}|^2$ , with and without mutual coupling.

#### A. Optimization of MiLAC With Mutual Coupling

In the presence of mutual coupling, the received signal power maximization problem is given by

$$\max_{\mathbf{B}} P_T |\mathbf{h}\mathbf{f}|^2 \quad (61)$$

$$\text{s.t. } \mathbf{f} = \left[ \left( \frac{\mathbf{Y}}{Y_0} + \begin{bmatrix} 1 & \mathbf{0} \\ \mathbf{0} & \mathbf{Y}_{TT} \end{bmatrix} \right)^{-1} \right]_{2:N_T+1,1}, \quad (62)$$

$$\mathbf{Y} = j\mathbf{B}, \quad \mathbf{B} = \mathbf{B}^T, \quad (63)$$

where the optimization variable is the real symmetric matrix  $\mathbf{B}$ , which is the susceptance matrix of the MiLAC. In the following, we derive in closed-form a solution to problem (61)-(63) that is proved to be globally optimal.

We begin by introducing the auxiliary constant terms  $\hat{\mathbf{h}} \in \mathbb{C}^{1 \times (N_T+1)}$  as  $\hat{\mathbf{h}} = [1, \mathbf{h}]$ ,  $\hat{\mathbf{Y}}_{TT} \in \mathbb{C}^{(N_T+1) \times (N_T+1)}$  as  $\hat{\mathbf{Y}}_{TT} = \text{diag}(Y_0, \mathbf{Y}_{TT})$ , and  $\hat{\mathbf{e}} \in \mathbb{C}^{(N_T+1) \times 1}$  as  $\hat{\mathbf{e}} = [1, 0, \dots, 0]^T$ . Therefore, problem (61)-(63) can be equivalently rewritten as

$$\max_{\mathbf{B}} P_T Y_0^2 \left| \hat{\mathbf{h}} \left( j\mathbf{B} + \hat{\mathbf{Y}}_{TT} \right)^{-1} \hat{\mathbf{e}} \right|^2 \quad (64)$$

$$\text{s.t. } \mathbf{B} = \mathbf{B}^T, \quad (65)$$

which has the same form as the received signal power maximization problem in the presence of a fully-connected RIS with mutual coupling solved in [28, Section III] through a global optimal solution. In the following, we globally solve (64)-(65) following a similar solution to [28, Section III], inspired by the effect of the matching (or decoupling) network used in the context of RIS in [29].

We introduce the auxiliary variable  $\bar{\mathbf{B}} \in \mathbb{R}^{(N_T+1) \times (N_T+1)}$  as a function of  $\mathbf{B}$  as

$$\bar{\mathbf{B}} = Y_0 \Re\{\hat{\mathbf{Y}}_{TT}\}^{-1/2} \left( \mathbf{B} + \Im\{\hat{\mathbf{Y}}_{TT}\} \right) \Re\{\hat{\mathbf{Y}}_{TT}\}^{-1/2}, \quad (66)$$

which is a real matrix since  $\mathbf{B}$ ,  $\Im\{\hat{\mathbf{Y}}_{TT}\}$ , and  $\Re\{\hat{\mathbf{Y}}_{TT}\}^{-1/2}$  are real matrices. Therefore, by substituting

$$\mathbf{B} = \frac{1}{Y_0} \Re\{\hat{\mathbf{Y}}_{TT}\}^{1/2} \bar{\mathbf{B}} \Re\{\hat{\mathbf{Y}}_{TT}\}^{1/2} - \Im\{\hat{\mathbf{Y}}_{TT}\}, \quad (67)$$

which follows from (66), into (64), problem (64)-(65) is equivalently rewritten as

$$\begin{aligned} \max_{\bar{\mathbf{B}}} P_T Y_0^2 \left| \hat{\mathbf{h}} \Re\{\hat{\mathbf{Y}}_{TT}\}^{-1/2} \sqrt{Y_0} \right. \\ \left. \times (j\bar{\mathbf{B}} + Y_0 \mathbf{I})^{-1} \sqrt{Y_0} \Re\{\hat{\mathbf{Y}}_{TT}\}^{-1/2} \hat{\mathbf{e}} \right|^2 \end{aligned} \quad (68)$$

$$\text{s.t. } (66), \quad \mathbf{B} = \mathbf{B}^T. \quad (69)$$

Observe that constraint (69) means that  $\bar{\mathbf{B}}$  can be an arbitrary symmetric matrix. Therefore, problem (68)-(69) can be solved for a symmetric matrix  $\bar{\mathbf{B}}$  and then  $\mathbf{B}$  can be derived with (67). To do so, we equivalently rewrite problem (68)-(69) as

$$\max_{\bar{\mathbf{B}}} P_T Y_0^3 \left| \hat{\mathbf{h}} \Re\{\hat{\mathbf{Y}}_{TT}\}^{-1/2} (j\bar{\mathbf{B}} + Y_0 \mathbf{I})^{-1} \hat{\mathbf{e}} \right|^2 \quad (70)$$

$$\text{s.t. } \bar{\mathbf{B}} = \bar{\mathbf{B}}^T, \quad (71)$$

where we also exploited the fact that  $\sqrt{Y_0} \Re\{\hat{\mathbf{Y}}_{TT}\}^{-1/2} \hat{\mathbf{e}} = \hat{\mathbf{e}}$ .

We now introduce another auxiliary variable  $\bar{\Theta} \in \mathbb{C}^{(N_T+1) \times (N_T+1)}$  as a function of  $\bar{\mathbf{B}}$  as

$$\bar{\Theta} = (Y_0 \mathbf{I} + j\bar{\mathbf{B}})^{-1} (Y_0 \mathbf{I} - j\bar{\mathbf{B}}), \quad (72)$$

which helps in solving (70)-(71) because of the following two properties. First, as a direct consequence of (72), we have the relationship  $(j\bar{\mathbf{B}} + Y_0 \mathbf{I})^{-1} = (\bar{\Theta} + \mathbf{I}) / (2Y_0)$ , useful to simplify the objective function in (70). Second, since  $\bar{\mathbf{B}}$  can be an arbitrary symmetric matrix,  $\bar{\Theta}$  can be an arbitrary unitary and symmetric matrix, from which  $\bar{\mathbf{B}}$  can be recovered by inverting (72). These two properties allow us to rewrite (70)-(71) as

$$\max_{\bar{\Theta}} \frac{P_T Y_0}{4} \left| \hat{\mathbf{h}} \Re\{\hat{\mathbf{Y}}_{TT}\}^{-1/2} (\bar{\Theta} + \mathbf{I}) \hat{\mathbf{e}} \right|^2 \quad (73)$$

$$\text{s.t. } \bar{\Theta}^H \bar{\Theta} = \mathbf{I}, \quad \bar{\Theta} = \bar{\Theta}^T, \quad (74)$$

which can be further simplified as

$$\max_{\bar{\Theta}} \frac{P_T Y_0}{4} \left| \hat{\mathbf{h}} \Re\{\mathbf{Y}_{TT}\}^{-1/2} [\bar{\Theta}]_{2:N_T+1,1} \right|^2 \quad (75)$$

$$\text{s.t. } \bar{\Theta}^H \bar{\Theta} = \mathbf{I}, \quad \bar{\Theta} = \bar{\Theta}^T, \quad (76)$$

because of the definitions of  $\hat{\mathbf{h}}$ ,  $\hat{\mathbf{Y}}_{TT}$ , and  $\hat{\mathbf{e}}$ . As discussed in [12], the global optimal solution to this problem ensures that  $[\bar{\Theta}]_{2:N_T+1,1} = (\mathbf{h} \Re\{\mathbf{Y}_{TT}\}^{-1/2})^H / \|\mathbf{h} \Re\{\mathbf{Y}_{TT}\}^{-1/2}\|$ , up to a phase shift. A unitary symmetric matrix  $\bar{\Theta}$  fulfilling this

condition is given as a function of the right singular vectors of  $\mathbf{h}\Re\{\mathbf{Y}_{TT}\}^{-1/2}$ , collected into the columns of a matrix denoted as  $\mathbf{V} \in \mathbb{C}^{N_T \times N_T}$ . Partitioning  $\mathbf{V}$  as  $\mathbf{V} = [\bar{\mathbf{v}}, \bar{\mathbf{V}}]$ , with  $\bar{\mathbf{v}} \in \mathbb{C}^{N_T \times 1}$  and  $\bar{\mathbf{V}} \in \mathbb{C}^{N_T \times (N_T-1)}$ , an optimal  $\bar{\Theta}$  is given by

$$\bar{\Theta} = \begin{bmatrix} 0 & \bar{\mathbf{v}}^T \\ \bar{\mathbf{v}} & \bar{\mathbf{V}}\bar{\mathbf{V}}^T \end{bmatrix}, \quad (77)$$

which is unitary and symmetric by construction.

The maximum received signal power achieved by MiLAC-aided beamforming with mutual coupling is given by substituting  $[\bar{\Theta}]_{2:N_T+1,1} = (\mathbf{h}\Re\{\mathbf{Y}_{TT}\}^{-1/2})^H / \|\mathbf{h}\Re\{\mathbf{Y}_{TT}\}^{-1/2}\|$  into (75), giving

$$P_{\text{MC}}^{\text{MiLAC}} = \frac{P_T Y_0}{4} \left\| \mathbf{h}\Re\{\mathbf{Y}_{TT}\}^{-1/2} \right\|^2 \quad (78)$$

$$= \frac{P_T Y_0}{16} \mathbf{z}_{RT} \mathbf{Y}_{TT} \Re\{\mathbf{Y}_{TT}\} \mathbf{Y}_{TT}^H \mathbf{z}_{RT}^H, \quad (79)$$

where (79) follows from  $\mathbf{h} = \mathbf{z}_{RT} \mathbf{Y}_{TT} / 2$  and since  $\|\mathbf{v}\|^2 = \mathbf{v}\mathbf{v}^H$  for any row vector  $\mathbf{v}$ . We now observe that

$$\begin{aligned} \mathbf{Y}_{TT} \Re\{\mathbf{Y}_{TT}\}^{-1} \mathbf{Y}_{TT}^H &= \\ &= \Re\{\mathbf{Y}_{TT}\} + \Im\{\mathbf{Y}_{TT}\} \Re\{\mathbf{Y}_{TT}\}^{-1} \Im\{\mathbf{Y}_{TT}\}, \end{aligned} \quad (80)$$

by using  $\mathbf{Y}_{TT} = \Re\{\mathbf{Y}_{TT}\} + j\Im\{\mathbf{Y}_{TT}\}$ , which can be more concisely rewritten as

$$\mathbf{Y}_{TT} \Re\{\mathbf{Y}_{TT}\}^{-1} \mathbf{Y}_{TT}^H = \Re\{\mathbf{Z}_{TT}\}^{-1}, \quad (81)$$

by exploiting  $(\mathbf{A} + j\mathbf{B})^{-1} = (\mathbf{A} + \mathbf{B}\mathbf{A}^{-1}\mathbf{B})^{-1} + j\mathbf{A}^{-1}\mathbf{B}(\mathbf{A} + \mathbf{B}\mathbf{A}^{-1}\mathbf{B})^{-1}$ , with  $\mathbf{A}$  and  $\mathbf{B}$  being square real matrices [30]. Therefore, substituting (81) into (79), we obtain

$$P_{\text{MC}}^{\text{MiLAC}} = \frac{P_T Y_0}{16} \mathbf{z}_{RT} \Re\{\mathbf{Z}_{TT}\}^{-1} \mathbf{z}_{RT}^H \quad (82)$$

$$= \frac{P_T Y_0}{16} \left\| \mathbf{z}_{RT} \Re\{\mathbf{Z}_{TT}\}^{-1/2} \right\|^2, \quad (83)$$

as the received signal power achievable by a MiLAC in a MISO system with mutual coupling.

We want now to derive the average performance  $\mathbb{E}[P_{\text{MC}}^{\text{MiLAC}}]$  under the assumption that  $\mathbf{z}_{RT}$  is a random variable with covariance matrix  $\mathbb{E}[\mathbf{z}_{RT}^H \mathbf{z}_{RT}] = \rho \mathbf{I}$ , i.e., in the presence of uncorrelated fading with path gain  $\rho$ . By taking the expectation of (82), we obtain

$$\mathbb{E}[P_{\text{MC}}^{\text{MiLAC}}] = \frac{P_T Y_0}{16} \mathbb{E}[\mathbf{z}_{RT} \Re\{\mathbf{Z}_{TT}\}^{-1} \mathbf{z}_{RT}^H] \quad (84)$$

$$= \frac{P_T Y_0 \rho}{16} \text{Tr}(\Re\{\mathbf{Z}_{TT}\}^{-1}), \quad (85)$$

where (85) follows from the symmetry of the Frobenius inner product, the linearity of the trace, and the assumption that  $\mathbb{E}[\mathbf{z}_{RT}^H \mathbf{z}_{RT}] = \rho \mathbf{I}$ . Interestingly, the average received signal power scales only with the trace term  $\text{Tr}(\Re\{\mathbf{Z}_{TT}\}^{-1})$ , and depends only on the real part of the mutual coupling matrix.

### B. Optimization of MiLAC With No Mutual Coupling

We now show how the proposed optimization and performance analysis simplifies under the assumptions of perfect matching at all transmitting antennas and no mutual coupling,

i.e.,  $\mathbf{Z}_{TT} = Z_0 \mathbf{I}$ , or, equivalently,  $\mathbf{Y}_{TT} = Y_0 \mathbf{I}$ . In this case, the received signal power maximization problem is

$$\max_{\mathbf{B}} P_T |\mathbf{h}\mathbf{f}|^2 \quad (86)$$

$$\text{s.t. } \mathbf{f} = \left[ \left( \frac{\mathbf{Y}}{Y_0} + \mathbf{I} \right)^{-1} \right]_{2:N_T+1,1}, \quad (87)$$

$$\mathbf{Y} = j\mathbf{B}, \quad \mathbf{B} = \mathbf{B}^T, \quad (88)$$

where  $\mathbf{B}$  is the susceptance of the MiLAC, which is real and symmetric.

A globally optimal solution to (86)-(88) can be found by introducing the scattering matrix of the MiLAC  $\Theta \in \mathbb{C}^{(N_T+1) \times (N_T+1)}$  as a function of  $\mathbf{B}$  as

$$\Theta = (Y_0 \mathbf{I} + j\mathbf{B})^{-1} (Y_0 \mathbf{I} - j\mathbf{B}), \quad (89)$$

which is unitary and symmetric. By exploiting the relationship  $(j\mathbf{B}/Y_0 + \mathbf{I})^{-1} = (\Theta + \mathbf{I})/2$ , (86)-(88) can be rewritten as

$$\max_{\Theta} \frac{P_T}{4} \left| \mathbf{h}[\Theta]_{2:N_T+1,1} \right|^2 \quad (90)$$

$$\text{s.t. } \Theta^H \Theta = \mathbf{I}, \quad \Theta = \Theta^T, \quad (91)$$

which has a global optimal solution as discussed in [12]. Given the matrix  $\mathbf{U} \in \mathbb{C}^{N_T \times N_T}$  containing the right singular vectors of  $\mathbf{h}$  in its columns, partitioned as  $\mathbf{U} = [\bar{\mathbf{u}}, \bar{\mathbf{U}}]$ , with  $\bar{\mathbf{u}} \in \mathbb{C}^{N_T \times 1}$  and  $\bar{\mathbf{U}} \in \mathbb{C}^{N_T \times (N_T-1)}$ , it is possible to show that an optimal  $\Theta$  is

$$\Theta = \begin{bmatrix} 0 & \bar{\mathbf{u}}^T \\ \bar{\mathbf{u}} & \bar{\mathbf{U}}\bar{\mathbf{U}}^T \end{bmatrix}, \quad (92)$$

which ensures that  $[\Theta]_{2:N_T+1,1} = \mathbf{h}^H / \|\mathbf{h}\|$ .

The maximum received signal power achievable by a MiLAC with no mutual coupling can be readily obtained by substituting  $[\Theta]_{2:N_T+1,1} = \mathbf{h}^H / \|\mathbf{h}\|$  into (90), which gives

$$P_{\text{NoMC}}^{\text{MiLAC}} = \frac{P_T}{4} \|\mathbf{h}\|^2 \quad (93)$$

$$= \frac{P_T Y_0^2}{16} \|\mathbf{z}_{RT}\|^2, \quad (94)$$

where (94) follows from  $\mathbf{h} = \mathbf{z}_{RT} / (2Z_0)$ . Note that  $P_{\text{NoMC}}^{\text{MiLAC}}$  can also be obtained by substituting  $\mathbf{Z}_{TT} = Z_0 \mathbf{I}$  into the expression of  $P_{\text{MC}}^{\text{MiLAC}}$  in (83), as expected.

We now derive the average performance  $\mathbb{E}[P_{\text{NoMC}}^{\text{MiLAC}}]$  under the assumption that  $\mathbf{z}_{RT}$  is a random variable with covariance matrix  $\mathbb{E}[\mathbf{z}_{RT}^H \mathbf{z}_{RT}] = \rho \mathbf{I}$ . Taking the expectation of (94), we have

$$\mathbb{E}[P_{\text{NoMC}}^{\text{MiLAC}}] = \frac{P_T Y_0^2}{16} \mathbb{E}[\mathbf{z}_{RT} \mathbf{z}_{RT}^H] \quad (95)$$

$$= \frac{P_T Y_0^2 \rho}{16} N_T, \quad (96)$$

following the symmetry of the Frobenius inner product, the linearity of the trace, and applying our assumption  $\mathbb{E}[\mathbf{z}_{RT}^H \mathbf{z}_{RT}] = \rho \mathbf{I}$ . Observe that the received signal power scales with the number of antennas  $N_T$ , as for a digital MISO system operating maximum ratio transmission (MRT).

To analyze the impact of mutual coupling on MiLAC-aided systems, we present the following result comparing the average performance of MiLAC with and without mutual coupling.

TABLE I  
COMPARISON BETWEEN MiLAC-AIDED AND DIGITAL MISO SYSTEMS.

	MiLAC	Digital with matching network	Digital without matching network
# of RF chains	1	$N_T$	$N_T$
DACs resolution	Low	High	High
# of impedance components	$\mathcal{O}(N_T)$	$\mathcal{O}(N_T^2)$	0
Type of impedance components	Tunable	Fixed	None
Operations at each symbol time	0	$\mathcal{O}(N_T)$	$\mathcal{O}(N_T)$
$P$ with mutual coupling	$\frac{P_T Y_0}{16} \ \mathbf{z}_{RT} \Re\{\mathbf{Z}_{TT}\}^{-1/2}\ ^2$	$\frac{P_T Y_0}{16} \ \mathbf{z}_{RT} \Re\{\mathbf{Z}_{TT}\}^{-1/2}\ ^2$	$\frac{P_T}{4} \ \mathbf{z}_{RT} (\mathbf{Z}_{TT} + Z_0 \mathbf{I})^{-1}\ ^2$
$\mathbb{E}[P]$ with mutual coupling	$\frac{P_T Y_0 \rho}{16} \text{Tr}(\Re\{\mathbf{Z}_{TT}\}^{-1})$	$\frac{P_T Y_0 \rho}{16} \text{Tr}(\Re\{\mathbf{Z}_{TT}\}^{-1})$	$\frac{P_T \rho}{4} \text{Tr}\left(\left((\mathbf{Z}_{TT} + Z_0 \mathbf{I})^H (\mathbf{Z}_{TT} + Z_0 \mathbf{I})\right)^{-1}\right)$
$P$ without mutual coupling	$\frac{P_T Y_0^2}{16} \ \mathbf{z}_{RT}\ ^2$	$\frac{P_T Y_0^2}{16} \ \mathbf{z}_{RT}\ ^2$	$\frac{P_T Y_0^2}{16} \ \mathbf{z}_{RT}\ ^2$
$\mathbb{E}[P]$ without mutual coupling	$\frac{P_T Y_0^2 \rho}{16} N_T$	$\frac{P_T Y_0^2 \rho}{16} N_T$	$\frac{P_T Y_0^2 \rho}{16} N_T$

**Proposition 1.** *With uncorrelated fading, i.e., when  $\mathbb{E}[\mathbf{z}_{RT}^H \mathbf{z}_{RT}] = \rho \mathbf{I}$ , mutual coupling between the MiLAC antennas improves the average received signal power, i.e.,*

$$\mathbb{E}[P_{MC}^{MiLAC}] \geq \mathbb{E}[P_{NoMC}^{MiLAC}]. \quad (97)$$

*Proof.* Recalling that  $\mathbb{E}[P_{MC}^{MiLAC}]$  and  $\mathbb{E}[P_{NoMC}^{MiLAC}]$  are given by (85) and (96), proving this proposition requires to show that  $\text{Tr}(\Re\{\mathbf{Z}_{TT}\}^{-1}) \geq Y_0 N_T$ . This directly follows from [28, Lemma 1], which is applicable since  $\Re\{\mathbf{Z}_{TT}\}$  is a positive definite matrix with diagonal elements  $[\Re\{\mathbf{Z}_{TT}\}]_{n,n} = 1/Y_0$ , considering perfect antenna matching.  $\square$

Interestingly, MiLAC can constructively exploit mutual coupling to enhance the received signal power. It can be interpreted as a reconfigurable matching network that adapts to the channel realization, thereby performing beamforming while exploiting the effects of mutual coupling.

## VII. COMPARISON WITH DIGITAL BEAMFORMING

Considering a MiLAC-aided MISO system with mutual coupling, we have derived a global optimal solution for the MiLAC and characterized its performance limits in closed form. In this section, we compare the performance of MiLAC-aided beamforming with digital beamforming, considering the two cases when the digital transmitter is equipped with a matching network or not, as shown in Fig. 5(b) and (c), respectively.

### A. Digital Beamforming With Matching Network

The considered MISO system with MiLAC at the transmitter in Fig. 5(a) can be compared with an equivalent MISO system operating digital beamforming with a matching network, as shown in Fig. 5(b). Following the system model derived in Section III with  $N_R = 1$  antenna at the receiver, which is assumed to be perfectly matched, i.e.,  $z_{RR} = Z_0$ , we have that the received signal  $z$  writes as

$$z = \mathbf{h}\mathbf{s}, \quad (98)$$

where  $\mathbf{s}$  is the transmitted signal such that  $\mathbb{E}[\|\mathbf{s}\|^2] = P_T$ , with  $P_T$  being the transmitted signal power, and  $\mathbf{h}$  is given as a function of the matching network impedance matrix  $\mathbf{Z}_F$  by

$$\mathbf{h} = \frac{1}{2} \mathbf{z}_{RT} \mathbf{J}_T^T (\mathbf{Z}_T + Z_0 \mathbf{I})^{-1}, \quad (99)$$

where  $\mathbf{Z}_T$  and  $\mathbf{J}_T$  are defined in (30) and (31), respectively. According to [18, Section V], it is convenient to fix the impedance matrix of the matching network to

$$\mathbf{Z}_F = \begin{bmatrix} \mathbf{0} & -j\sqrt{Z_0} \Re\{\mathbf{Z}_{TT}\}^{1/2} \\ -j\sqrt{Z_0} \Re\{\mathbf{Z}_{TT}\}^{1/2} & -j\Im\{\mathbf{Z}_{TT}\} \end{bmatrix}, \quad (100)$$

as a function of the mutual coupling matrix  $\mathbf{Z}_{TT}$ , such that all the power is delivered from the generators to the antennas. Substituting (100) into (30) and (31), we obtain  $\mathbf{Z}_T = Z_0 \mathbf{I}$  and  $\mathbf{J}_T = -j\sqrt{Z_0} \Re\{\mathbf{Z}_{TT}\}^{-1/2}$ , yielding

$$\mathbf{h} = -\frac{j}{4\sqrt{Z_0}} \mathbf{z}_{RT} \Re\{\mathbf{Z}_{TT}\}^{-1/2}. \quad (101)$$

The received power is maximized with MRT, which gives

$$P_{MC}^{\text{Matching}} = P_T \|\mathbf{h}\|^2 \quad (102)$$

$$= \frac{P_T Y_0}{16} \left\| \mathbf{z}_{RT} \Re\{\mathbf{Z}_{TT}\}^{-1/2} \right\|^2, \quad (103)$$

where (103) follows from (101).

Comparing the performance of MiLAC-aided beamforming in (83) with the performance of digital beamforming with a matching network, we readily obtain the following result.

**Proposition 2.** *MiLAC achieves the same received power as digital beamforming with matching network for any channel realization  $\mathbf{z}_{RT}$ , i.e.,  $P_{MC}^{MiLAC} = P_{MC}^{\text{Matching}}$ .*

A detailed comparison between MiLAC-aided beamforming and digital beamforming with a matching network is reported in Table I. Following Proposition 2, these two strategies achieve the same performance for any channel realization, both in the presence or in the absence of mutual coupling. There are however differences in terms of hardware implementation. A MiLAC only requires one RF chain to perform single-stream transmission, which can include low-resolution DACs since it only carries the transmitted symbol, lying in a constellation with finite cardinality. The number of impedance components required by a MiLAC serving a single-antenna user is  $2N_T + 1$ , scaling with  $\mathcal{O}(N_T)$ , because of the optimality of the stem-connected architecture proposed in [13], while the number of impedance components in a  $2N_T$ -port fully-connected matching network scales with  $\mathcal{O}(N_T^2)$ . MiLAC also does not require any computation at each symbol time, while the price to pay is that its microwave network includes tunable components, which are more challenging to implement than fixed ones.

### B. Digital Beamforming Without Matching Network

We now consider a digital MISO system without the matching network, as shown in Fig. 5(c). Following the system model derived in Section II with  $N_R = 1$  antenna at the receiver, which is assumed to be perfectly matched, i.e.,  $z_{RR} = Z_0$ , the received signal  $z$  writes as

$$z = \mathbf{h}s, \quad (104)$$

where  $s$  is the transmitted signal such that  $\mathbb{E}[\|s\|^2] = P_T$ , with  $P_T$  being the transmitted signal power, and  $\mathbf{h}$  is the wireless channel given by

$$\mathbf{h} = \frac{1}{2} \mathbf{z}_{RT} (\mathbf{Z}_{TT} + Z_0 \mathbf{I})^{-1}, \quad (105)$$

The received power is maximized with MRT, which gives

$$P_{MC}^{\text{Digital}} = P_T \|\mathbf{h}\|^2 \quad (106)$$

$$= \frac{P_T}{4} \left\| \mathbf{z}_{RT} (\mathbf{Z}_{TT} + Z_0 \mathbf{I})^{-1} \right\|^2. \quad (107)$$

where (107) follows from (105).

The following proposition compares the received signal power of MiLAC with that of digital beamforming with no matching network in the presence of mutual coupling.

**Proposition 3.** *With mutual coupling, MiLAC achieves higher received signal power than digital beamforming with no matching network for any channel realization  $\mathbf{z}_{RT}$ , i.e.,*

$$P_{MC}^{\text{MiLAC}} \geq P_{MC}^{\text{Digital}}. \quad (108)$$

*Proof.* Recalling that  $P_{MC}^{\text{MiLAC}}$  and  $P_{MC}^{\text{Digital}}$  are given by (83) and (107), proving this proposition requires to show that

$$\frac{Y_0}{4} \left\| \mathbf{z}_{RT} \Re\{\mathbf{Z}_{TT}\}^{-1/2} \right\|^2 \geq \left\| \mathbf{z}_{RT} (\mathbf{Z}_{TT} + Z_0 \mathbf{I})^{-1} \right\|^2, \quad (109)$$

for any  $\mathbf{z}_{RT} \in \mathbb{C}^{1 \times N_T}$ , which is the same as verifying the matrix inequality

$$\frac{Y_0}{4} \Re\{\mathbf{Z}_{TT}\}^{-1} \succcurlyeq \left( (\mathbf{Z}_{TT} + Z_0 \mathbf{I})^H (\mathbf{Z}_{TT} + Z_0 \mathbf{I}) \right)^{-1}. \quad (110)$$

Since for  $\mathbf{A}$  and  $\mathbf{B}$  positive definite,  $\mathbf{A} \succcurlyeq \mathbf{B}$  is the same as  $\mathbf{B}^{-1} \succcurlyeq \mathbf{A}^{-1}$ , our condition becomes

$$(\mathbf{Z}_{TT} + Z_0 \mathbf{I})^H (\mathbf{Z}_{TT} + Z_0 \mathbf{I}) \succcurlyeq 4Z_0 \Re\{\mathbf{Z}_{TT}\}, \quad (111)$$

which can be equivalently rewritten as

$$\mathbf{Z}_{TT}^H \mathbf{Z}_{TT} + 2Z_0 \Re\{\mathbf{Z}_{TT}\} + Z_0^2 \mathbf{I} \succcurlyeq 4Z_0 \Re\{\mathbf{Z}_{TT}\}. \quad (112)$$

Since saying  $\mathbf{A} \succcurlyeq \mathbf{B}$  is the same as saying  $\mathbf{A} - \mathbf{B} \succcurlyeq \mathbf{0}$ , our condition becomes

$$\mathbf{Z}_{TT}^H \mathbf{Z}_{TT} - 2Z_0 \Re\{\mathbf{Z}_{TT}\} + Z_0^2 \mathbf{I} \succcurlyeq \mathbf{0}, \quad (113)$$

which can be equivalently rewritten as

$$(\mathbf{Z}_{TT} - Z_0 \mathbf{I})^H (\mathbf{Z}_{TT} - Z_0 \mathbf{I}) \succcurlyeq \mathbf{0}, \quad (114)$$

which is always satisfied since  $(\mathbf{Z}_{TT} - Z_0 \mathbf{I})^H (\mathbf{Z}_{TT} - Z_0 \mathbf{I})$  is positive semi-definite.  $\square$

The equality in Proposition (3) is satisfied when  $\mathbf{Z}_{TT} = Z_0 \mathbf{I}$ , i.e., with perfect matching and no mutual coupling.

This implies that MiLAC performs as digital beamforming in a MISO system with perfect matching and no mutual coupling, in line with the results in [12]. Finally, the average performance  $\mathbb{E}[P_{MC}^{\text{Digital}}]$  in the case  $\mathbf{z}_{RT}$  has covariance matrix  $\mathbb{E}[\mathbf{z}_{RT}^H \mathbf{z}_{RT}] = \rho \mathbf{I}$ , i.e., in the presence of uncorrelated fading with path gain  $\rho$ , is readily given by taking the expectation of (107) as

$$\mathbb{E} \left[ P_{MC}^{\text{Digital}} \right] = \frac{P_T \rho}{4} \text{Tr} \left( \left( (\mathbf{Z}_{TT} + Z_0 \mathbf{I})^H (\mathbf{Z}_{TT} + Z_0 \mathbf{I}) \right)^{-1} \right). \quad (115)$$

The comprehensive comparison between MiLAC-aided and digital systems is summarized in Table I, which shows that the only benefits of digital beamforming with no matching network is that it does not require any RF component, and therefore reduced losses are expected in practical systems.

## VIII. NUMERICAL RESULTS

This section provides simulation results to validate the derived global optimal closed-form solutions and performance bounds for MiLAC with mutual coupling. Consider a MISO system with MiLAC at the transmitter. The antenna array of the MiLAC is a uniform planar array (UPA) of antennas located in the  $x$ - $y$  plane, with dimensions  $N_X \times N_Y$ , where  $N_X = 8$  and  $N_Y = N_T/8$ , and with antenna spacing  $d$ . The antennas are thin wire dipoles parallel to the  $y$  axis with length  $\ell = \lambda/4$  and radius  $r \ll \ell$ , where  $\lambda = c/f$  is the wavelength of the frequency  $f = 28$  GHz, and  $c$  is the speed of light. All the antennas are assumed to be perfectly matched to  $Z_0 = 50 \Omega$ , giving  $[\mathbf{Z}_{TT}]_{n,n} = Z_0$ , for  $n = 1, \dots, N_T$ . In addition, the  $(q, p)$ th entry of  $\mathbf{Z}_{TT}$ , with  $q \neq p$ , represent the mutual coupling between the antenna  $p$  located in  $(x_p, y_p)$  and the antenna  $q$  located in  $(x_q, y_q)$ . Following [22], the entry  $[\mathbf{Z}_{TT}]_{q,p} = [\mathbf{Z}_{TT}]_{p,q}$  is modeled as

$$\begin{aligned} [\mathbf{Z}_{TT}]_{q,p} &= \int_{y_q - \frac{\ell}{2}}^{y_q + \frac{\ell}{2}} \int_{y_p - \frac{\ell}{2}}^{y_p + \frac{\ell}{2}} \frac{j\eta_0}{4\pi k_0} \left( \frac{(y'' - y')^2}{d_{q,p}^2} \right) \\ &\times \left( \frac{3}{d_{q,p}^2} + \frac{3jk_0}{d_{q,p}} - k_0^2 \right) - \frac{jk_0 + d_{q,p}^{-1} + k_0^2}{d_{q,p}} \frac{e^{-jk_0 d_{q,p}}}{d_{q,p}} \\ &\times \frac{\sin(k_0(\frac{\ell}{2} - |y' - y_p|)) \sin(k_0(\frac{\ell}{2} - |y'' - y_q|))}{\sin^2(k_0 \frac{\ell}{2})} dy' dy'', \end{aligned} \quad (116)$$

where  $\eta_0 = 377 \Omega$  is the impedance of free space,  $k_0 = 2\pi/\lambda$  is the wavenumber, and  $d_{q,p} = \sqrt{(x_q - x_p)^2 + (y'' - y')^2}$ . We generate  $\mathbf{z}_{RT}$  as independent Rayleigh distributed with unit path gain, i.e.,  $\mathbf{z}_{RT} \sim \mathcal{CN}(\mathbf{0}, \mathbf{I})$ . We consider unit path gain and unit transmit signal power, i.e.,  $\rho = 1$  and  $P_T = 1$ , for simplicity, since they impact the received signal power by just scaling it by a constant factor.

In Fig. 6, we report the received signal power obtained by MiLAC with mutual coupling for different values of antenna spacing  $d \in [\lambda/2, \lambda/3, \lambda/4]$ , and without mutual coupling, i.e., with  $\mathbf{Z}_{TT} = Z_0 \mathbf{I}$ . We compare the following three baselines.

- Optim.: The average received signal power resulting from Monte Carlo simulations, where at each channel

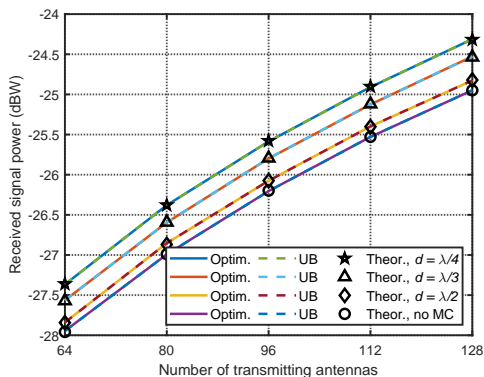


Fig. 6. Received signal power versus the number of transmitting antennas achieved by MiLAC.

realization the MiLAC is optimized with the proposed algorithm in Section VI.

- UB: The average received signal power resulting from Monte Carlo simulations, where at each channel realization the received signal power is given by its upper bound  $P_{MC}^{\text{MiLAC}} = P_T Y_0 \| \mathbf{z}_{RT} \Re \{ \mathbf{Z}_{TT} \}^{-1/2} \|^2 / 16$  or  $P_{\text{NoMC}}^{\text{MiLAC}} = P_T Y_0^2 \| \mathbf{z}_{RT} \|^2 / 16$ .
- Theor.: The theoretical average received signal power given by  $\mathbb{E}[P_{MC}^{\text{MiLAC}}] = P_T Y_0 \rho \text{Tr}(\Re \{ \mathbf{Z}_{TT} \}^{-1}) / 16$  or  $\mathbb{E}[P_{\text{NoMC}}^{\text{MiLAC}}] = P_T Y_0^2 \rho N_T / 16$ .

We make the following four observations from Fig. 6. *First*, the MiLAC optimized with the proposed solution exactly achieves the received signal power upper bound, confirming the effectiveness of our global optimal closed-form solution. *Second*, the average received signal power obtained with Monte Carlo simulations exactly corresponds to the theoretical average derived in closed form, confirming the validity of our closed-form scaling laws. *Third*, the presence of mutual coupling allows the MiLAC to achieve higher received signal power than with no mutual coupling, confirming Proposition 1. A similar trend was also analytically proved for RIS-aided systems in [28]. *Fourth*, when  $d = \lambda$ , the mutual coupling is so weak that the achieved performance is approximately the same as in the absence of mutual coupling.

We extend the comparison to include systems where the MiLAC is optimized without accounting for mutual coupling. In Fig. 7, we report the received signal power achieved by the MiLAC, when it is optimized through mutual coupling aware as well as unaware algorithms, for different numbers of antennas  $N_T \in [64, 96, 128]$ . For MiLAC re-configured with mutual coupling aware optimization, the performance is given by the received signal power upper bound  $P_{MC}^{\text{MiLAC}} = P_T Y_0 \| \mathbf{z}_{RT} \Re \{ \mathbf{Z}_{TT} \}^{-1/2} \|^2 / 16$  or  $P_{\text{NoMC}}^{\text{MiLAC}} = P_T Y_0^2 \| \mathbf{z}_{RT} \|^2 / 16$ . For MiLAC optimized in a mutual coupling unaware fashion, we assume that  $\mathbf{Z}_{II} = Z_0 \mathbf{I}$  during the optimization phase, and optimize the MiLAC by using the solution proposed in Section VI-B. From the obtained  $\Theta$ , the susceptance matrix  $\mathbf{B}$  is obtained by inverting (89), and it is plugged into the channel model with mutual coupling in (58)-(59) to get the received signal power of a MiLAC-aided system with mutual coupling unaware optimization.

We make the following three remarks from Fig. 7. *First*,

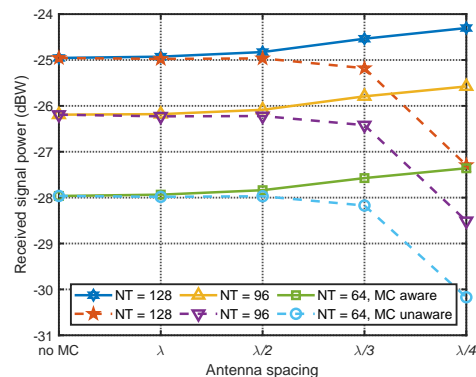


Fig. 7. Received signal power versus the antenna spacing achieved by MiLAC.

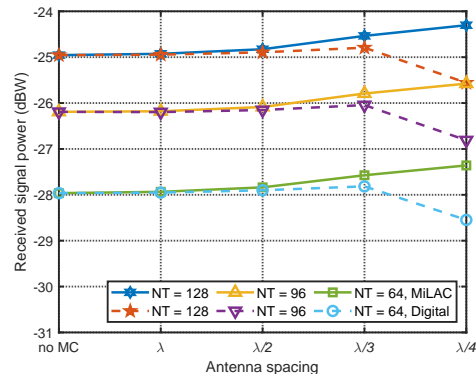


Fig. 8. Received signal power versus the antenna spacing achieved by MiLAC and digital beamforming with no matching network.

when optimizing the MiLAC accounting for mutual coupling, the performance increases with the mutual coupling strength, i.e., as the antenna spacing decreases. This is because MiLAC can effectively deliver the power to the coupled antennas, as a matching network. However, when the MiLAC is optimized not being aware of the mutual coupling, its performance dramatically drops for small values of antenna spacing, experiencing a degradation of up to 3 dB. This is because the MiLAC is optimized based on a channel model with no mutual coupling, which differs from the physics-compliant channel model with the mutual coupling effects. *Second*, the impact of mutual coupling can be approximately neglected during the optimization when the antenna spacing is larger than half-wavelength, i.e.,  $d \geq \lambda/2$ . The MiLAC can be successfully optimized without considering mutual coupling in this case, given how weak the mutual coupling is. *Third*, the above remarks are independent of the number of antennas  $N_T$ .

We finally compare MiLAC with digital beamforming with no matching network in the presence of mutual coupling. In Fig. 8, we report the received signal power achieved by MiLAC (optimized through the proposed globally optimal solution) and by digital beamforming (assuming MRT, which is optimal in MISO). For MiLAC, the performance is given by the received signal power upper bound  $P_{MC}^{\text{MiLAC}} = P_T Y_0 \| \mathbf{z}_{RT} \Re \{ \mathbf{Z}_{TT} \}^{-1/2} \|^2 / 16$  or  $P_{\text{NoMC}}^{\text{MiLAC}} = P_T Y_0^2 \| \mathbf{z}_{RT} \|^2 / 16$ . For digital beamforming, the performance is given by the corresponding received signal power upper

bound  $P_{MC}^{\text{Digital}} = P_T \|\mathbf{z}_{RT}(\mathbf{Z}_{TT} + Z_0 \mathbf{I})^{-1}\|^2/4$  or  $P_{NoMC}^{\text{Digital}} = P_T Y_0^2 \|\mathbf{z}_{RT}\|^2/16$ . From Fig. 8, we observe that MiLAC-aided beamforming outperforms digital beamforming in the presence of mutual coupling, validating Proposition 3. A MiLAC can outperform digital beamforming since it acts as a reconfigurable matching network which can simultaneously maximize the power flow from the RF chain to the antennas and perform beamforming. The discrepancy between the two beamforming strategies increases with the mutual coupling strength (i.e., as the antenna spacing decreases), while it vanishes in the absence of mutual coupling, in agreement with [12].

## IX. CONCLUSION

We have developed a rigorous physics-compliant modeling for MiLAC-aided MIMO systems by leveraging multiport network theory. Specifically, we have derived end-to-end system models for conventional digital MIMO and MiLAC-aided systems, considering systems where the MiLAC is deployed at the transmitter, the receiver, or both. The resulting models reveal how mutual coupling between the antennas fundamentally alters the channel and the precoding and combining matrices implemented by the MiLAC.

Building on the developed models, we have addressed the optimization of MiLACs in the presence of mutual coupling. For a MiLAC-aided MISO system, we have derived a closed-form solution that maximizes the received signal power under lossless and reciprocal constraints, and proved its global optimality. We have further obtained closed-form expressions for the maximum achievable performance with and without mutual coupling, thereby showing that mutual coupling effects improve the performance in MiLAC-aided systems. In addition, we have compared the performance of MiLAC-aided with digital MIMO systems, with or without a matching network. Our analytical derivations show that MiLAC always performs as digital beamforming with a matching network, and always outperforms digital beamforming without a matching network. Numerical results validate our theoretical findings and confirm that the proposed MiLAC optimization achieves the derived performance upper bounds, visibly outperforming digital MIMO systems when they are not equipped with a matching network.

## REFERENCES

- [1] M. Giordani, M. Polese, M. Mezzavilla, S. Rangan, and M. Zorzi, "Toward 6G networks: Use cases and technologies," *IEEE Commun. Mag.*, vol. 58, no. 3, pp. 55–61, 2020.
- [2] E. G. Larsson, O. Edfors, F. Tufvesson, and T. L. Marzetta, "Massive MIMO for next generation wireless systems," *IEEE Commun. Mag.*, vol. 52, no. 2, pp. 186–195, 2014.
- [3] E. Björnson, F. Kara, N. Kolomvakis, A. Kosasih, P. Ramezani, and M. B. Salman, "Enabling 6G performance in the upper mid-band by transitioning from massive to gigantic MIMO," *IEEE Open J. Commun. Soc.*, vol. 6, pp. 5450–5463, 2025.
- [4] F. Sahrabi and W. Yu, "Hybrid digital and analog beamforming design for large-scale antenna arrays," *IEEE J. Sel. Top. Signal Process.*, vol. 10, no. 3, pp. 501–513, 2016.
- [5] A. F. Molisch, V. V. Ratnam, S. Han, Z. Li, S. L. H. Nguyen, L. Li, and K. Haneda, "Hybrid beamforming for massive MIMO: A survey," *IEEE Commun. Mag.*, vol. 55, no. 9, pp. 134–141, 2017.
- [6] Q. Wu, S. Zhang, B. Zheng, C. You, and R. Zhang, "Intelligent reflecting surface-aided wireless communications: A tutorial," *IEEE Trans. Commun.*, vol. 69, no. 5, pp. 3313–3351, 2021.
- [7] N. Shlezinger, O. Dicker, Y. C. Eldar, I. Yoo, M. F. Imani, and D. R. Smith, "Dynamic metasurface antennas for uplink massive MIMO systems," *IEEE Trans. Commun.*, vol. 67, no. 10, pp. 6829–6843, 2019.
- [8] A. Silva, F. Monticone, G. Castaldi, V. Galdi, A. Alù, and N. Engheta, "Performing mathematical operations with metamaterials," *Science*, vol. 343, no. 6167, pp. 160–163, 2014.
- [9] D. Ielmini and H.-S. P. Wong, "In-memory computing with resistive switching devices," *Nature electronics*, vol. 1, no. 6, pp. 333–343, 2018.
- [10] M. Nerini and B. Clerckx, "Analog computing for signal processing and communications – Part I: Computing with microwave networks," *IEEE Trans. Signal Process.*, vol. 73, pp. 5183–5197, 2025.
- [11] M. Nerini and B. Clerckx, "Analog computing for signal processing and communications – Part II: Toward gigantic MIMO beamforming," *IEEE Trans. Signal Process.*, vol. 73, pp. 5198–5212, 2025.
- [12] M. Nerini and B. Clerckx, "Capacity of MIMO systems aided by microwave linear analog computers (MiLACs)," *arXiv preprint arXiv:2506.05983*, 2025.
- [13] M. Nerini and B. Clerckx, "MIMO systems aided by microwave linear analog computers: Capacity-achieving architectures with reduced circuit complexity," *arXiv preprint arXiv:2506.15052*, 2025.
- [14] T. Fang, X. Zhou, and Y. Mao, "On the performance of lossless reciprocal MiLAC architectures in multi-user networks," *arXiv preprint arXiv:2601.01834*, 2026.
- [15] Z. Wu, M. Nerini, and B. Clerckx, "Microwave linear analog computer (MiLAC)-aided multiuser MISO: Fundamental limits and beamforming design," *arXiv preprint arXiv:2601.10060*, 2026.
- [16] Q. Zhang, M. Nerini, and B. Clerckx, "Channel estimation in MIMO systems aided by microwave linear analog computers (MiLACs)," *arXiv preprint arXiv:2601.11438*, 2026.
- [17] B. Clerckx, C. Craeye, D. Vanhoenacker-Janvier, and C. Oestges, "Impact of antenna coupling on  $2 \times 2$  MIMO communications," *IEEE Trans. Veh. Technol.*, vol. 56, no. 3, pp. 1009–1018, 2007.
- [18] M. T. Ivrlač and J. A. Nossek, "Toward a circuit theory of communication," *IEEE Trans. Circuits Syst. I: Regul. Pap.*, vol. 57, no. 7, pp. 1663–1683, 2010.
- [19] M. T. Ivrlač and J. A. Nossek, "The multiport communication theory," *IEEE Circuits Syst. Mag.*, vol. 14, no. 3, pp. 27–44, 2014.
- [20] J. Wallace and M. Jensen, "Mutual coupling in MIMO wireless systems: A rigorous network theory analysis," *IEEE Trans. Wireless Commun.*, vol. 3, no. 4, pp. 1317–1325, 2004.
- [21] J. Wallace and M. Jensen, "Termination-dependent diversity performance of coupled antennas: Network theory analysis," *IEEE Trans. Antennas Propag.*, vol. 52, no. 1, pp. 98–105, 2004.
- [22] G. Gradoni and M. Di Renzo, "End-to-end mutual coupling aware communication model for reconfigurable intelligent surfaces: An electromagnetic-compliant approach based on mutual impedances," *IEEE Wireless Commun. Lett.*, vol. 10, no. 5, pp. 938–942, 2021.
- [23] S. Shen, B. Clerckx, and R. Murch, "Modeling and architecture design of reconfigurable intelligent surfaces using scattering parameter network analysis," *IEEE Trans. Wireless Commun.*, vol. 21, no. 2, pp. 1229–1243, 2022.
- [24] A. Abrardo, A. Toccafondi, and M. Di Renzo, "Design of reconfigurable intelligent surfaces by using S-parameter multiport network theory—optimization and full-wave validation," *IEEE Trans. Wireless Commun.*, vol. 23, no. 11, pp. 17 084–17 102, 2024.
- [25] M. Nerini, S. Shen, H. Li, M. Di Renzo, and B. Clerckx, "A universal framework for multiport network analysis of reconfigurable intelligent surfaces," *IEEE Trans. Wireless Commun.*, vol. 23, no. 10, pp. 14 575–14 590, 2024.
- [26] R. J. Williams, P. Ramírez-Espinosa, J. Yuan, and E. de Carvalho, "Electromagnetic based communication model for dynamic metasurface antennas," *IEEE Trans. Wireless Commun.*, vol. 21, no. 10, pp. 8616–8630, 2022.
- [27] D. M. Pozar, *Microwave engineering*. John Wiley & Sons, 2011.
- [28] M. Nerini, H. Li, and B. Clerckx, "Global optimal closed-form solutions for intelligent surfaces with mutual coupling: Is mutual coupling detrimental or beneficial?" *IEEE Trans. Wireless Commun.*, vol. 25, pp. 3201–3214, 2026.
- [29] D. Semmler, J. A. Nossek, M. Joham, B. Böck, and W. Utschick, "Decoupling networks and super-quadratic gains for RIS systems with mutual coupling," *IEEE Trans. Wireless Commun.*, vol. 25, pp. 1624–1639, 2026.
- [30] Z. Dai, L.-H. Lim, and K. Ye, "Complex matrix inversion via real matrix inversions," *Numerische Mathematik*, vol. 156, no. 6, pp. 2179–2219, 2024.